Journal of Organometallic Chemistry 849-850 (2017) 237–255

Contents lists available at ScienceDirect

Journal of Organometallic Chemistry

journal homepage: www.elsevier.com/locate/jorganchem

Syntheses and structures of square planar diplatinum butadiynediyl complexes with two different monophosphine ligands on each terminus; probing the feasibility of a new type of inorganic atropisomerism☆

Sandip Dey[1], Tianyi Zhang, Nattamai Bhuvanesh, John A. Gladysz*

Department of Chemistry, Texas A&M University, P.O. Box 30012, College Station, TX 77842-3012, USA

ARTICLE INFO

Article history:
Received 7 January 2017
Received in revised form
24 April 2017
Accepted 4 May 2017
Available online 5 May 2017

Keywords:
Platinum
Phosphine ligands
sp carbon chains
Substitution
Hagihara coupling
Low temperature NMR
Crystallography

ABSTRACT

Reactions of *trans*-$(C_6F_5)(p\text{-tol}_3P)_2Pt(Cl)$ (**PtCl**) and R_2PhP (1.0 equiv; R = **a**/Me, **b**/*p*-*t*-BuC_6H_4, **c**/*p*-$MeOC_6H_4$, **d**/*n*-Pr; CH_2Cl_2/rt (**a**) or toluene/reflux (**b-d**)) give mainly *trans*-$(C_6F_5)(R_2PhP)(p\text{-tol}_3P)Pt(Cl)$ (**Pt′Cl-a-d**, 89-29%) and some disubstitution products *trans*-$(C_6F_5)(R_2PhP)_2Pt(Cl)$ (**Pt″Cl-a-d**, 4–13%). No substitution occurs with *t*-Bu_2PhP. However, $(cod)(C_6F_5)Pt(Cl)$ and *t*-Bu_2PhP (2.7 equiv; toluene/reflux) react to give *trans*-$(C_6F_5)(t\text{-Bu}_2PhP)_2Pt(Cl)$ (**Pt″Cl-e**, 64%), which upon treatment with *p*-tol_3P (1.0 equiv, toluene/reflux) yields *trans*-$(C_6F_5)(t\text{-Bu}_2PhP)(p\text{-tol}_3P)Pt(Cl)$ (**Pt′Cl-e**, 91%). Additions of excess butadiyne to **Pt′Cl-a-d** (CH_2Cl_2, cat. CuI, $HNEt_2$) afford the butadiynyl complexes *trans*-$(C_6F_5)(R_2PhP)(p\text{-tol}_3P)Pt(C{\equiv}C)_2H$ (**Pt′C$_4$H-a-d**, 36–77%), but **Pt′Cl-e** does not similarly react. Cross couplings of **Pt′Cl-a-c** and **Pt′C$_4$H-a-c** (cat. CuI, $HNEt_2$) give mixtures of diplatinum butadiynyl complexes in which the two unlike phosphine ligands scramble over all four positions (**PtC$_4$Pt**, **PtC$_4$Pt′-a-c**, **PtC$_4$Pt″-a-c**, **Pt′C$_4$Pt′-a-c**, **Pt′C$_4$Pt″-a-c**, **Pt″C$_4$Pt″-b**; TLC separable, 27-2% each). A modified coupling recipe is tested with **Pt′Cl-b,d** and **Pt′C$_4$H-b,d** (*t*-BuOK, KPF_6, cat. CuCl), and gives **Pt′C$_4$Pt′-b,d** (21–76%) with only traces of scrambling. Crystal structures of **Pt″Cl-e**, **Pt′C$_4$H-a**, **Pt′C$_4$Pt′-a-d**, and **PtC$_4$Pt″-b** are determined, and the endgroup/endgroup interactions analyzed. Low temperature NMR spectra do not reveal any dynamic processes.

1. Introduction

There is an extensive literature of complexes in which two square planar platinum(II) fragments cap butadiynediyl or -C≡C-C≡C- moieties [1–3]. There is also an extensive literature involving higher homologs with as many as 28 sp carbon atoms [1c,2-6]. However, there are a number of interesting properties or phenomena that are uniquely associated with shorter sp carbon bridges. For example, the platinum(II)/platinum(III) radical cations generated by one electron oxidations are much more stable at modest chain lengths [2a,b,e,7].

In a recent paper [8], we described a quest for atropisomers [9] derived from diplatinum ethynediyl or PtC≡CPt complexes [10]. The idea was that with appropriate substitution patterns, as exemplified in Scheme 1 with adducts that bear two different *trans* disposed monophosphine ligands on each platinum, it might be possible to separate enantiomers or diastereomers with an axis of chirality. Alternatively, slow interconversion could be established by NMR techniques. To date, these efforts have not resulted in a demonstration of atropisomerism. However, this is likely because the phosphine ligands initially employed were not bulky enough (e.g., X/Y = Ph/Me in **I**). Promising second generation targets are easily envisioned (e.g., X/Y = Ph/*t*-Bu or *i*-Pr/*o*-C_6H_4X).

In laying the groundwork for these studies, related complexes with longer PtC≡CC≡CPt bridges were also investigated. Although in retrospect there was little chance of detecting atropisomerism in such species, they provided valuable testing grounds for syntheses of coupling partners, such as platinum chloride complexes with the types of monophosphine ligands in Scheme 1, *trans*-$(Ar)(R_2PhP)(p\text{-tol}_3P)Pt(Cl)$ [11]. They also revealed problematic phosphine scrambling processes under certain coupling conditions, and

☆ *dedication:* "to our friend Rick Adams, a source of inspiration and counsel for over forty years".

* Corresponding author.
E-mail address: gladysz@mail.chem.tamu.edu (J.A. Gladysz).
[1] Current address: Chemistry Division, Bhabha Atomic Research Center, Mumbai 400 085, India.

http://dx.doi.org/10.1016/j.jorganchem.2017.05.006
0022-328X/

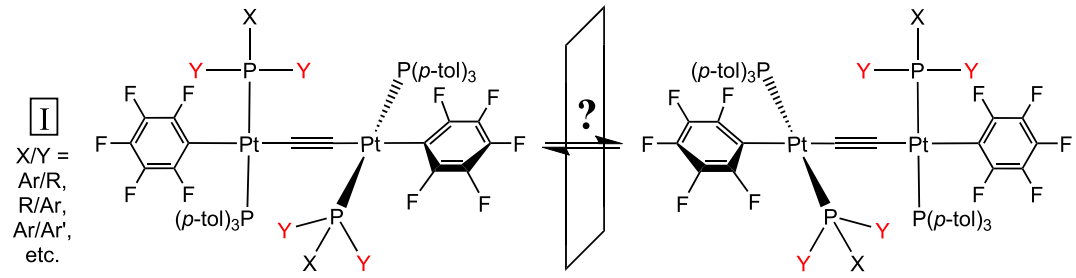

Scheme 1. Enantiomeric atropisomers derived from diplatinum ethynediyl complexes. The Y groups are diastereotopic and potentially distinguishable by NMR.

"standard" protocols that became unreliable in the presence of bulkier phosphine ligands. Furthermore, several crystal structures that help visualize the magnitudes of the endgroup/endgroup interactions, which must underpin any atropisomerism, could be determined. Accordingly, in this full paper, a detailed account of this previously undisclosed work is presented.

2. Results

2.1. Syntheses of monoplatinum complexes *trans*-(C_6F_5)(R_2PhP)(*p*-tol_3P)Pt(Cl)

The previously reported platinum chloride complex *trans*-(C_6F_5)(*p*-tol_3P)$_2$Pt(Cl) (**PtCl**) [2a] and Me_2PhP (1.0 equiv) were combined in CH_2Cl_2 at room temperature. As shown in Scheme 2 (top), workup gave the monosubstitution product *trans*-(C_6F_5)(Me_2PhP)(*p*-tol_3P)Pt(Cl) (**Pt′Cl-a**) as a white solid in 89% yield. In some cases, small amounts of **PtCl** remained, or the disubstituted byproduct *trans*-(C_6F_5)(Me_2PhP)$_2$Pt(Cl) (**Pt″Cl-a**) was detected (each ≤4%). In these cases, **Pt′Cl-a** was purified chromatographically. The identity of **Pt″Cl-a** was confirmed by an independent synthesis from [(C_6F_5)(tht)Pt(μ-Cl)]$_2$ and Me_2PhP (73%; Scheme 2, bottom). This route has been used to prepare many related platinum bis(phosphine) complexes [2a,c,5h,j].

Similar reactions were carried out with three other phosphines of the formula R_2PhP (R = alkyl or aryl; **b-d** in Scheme 2). With the triarylphosphines (*p*-*t*-BuC_6H_4)$_2$PhP and (*p*-$MeOC_6H_4$)$_2$PhP, no reactions with **PtCl** occurred over the course of 16 h in refluxing

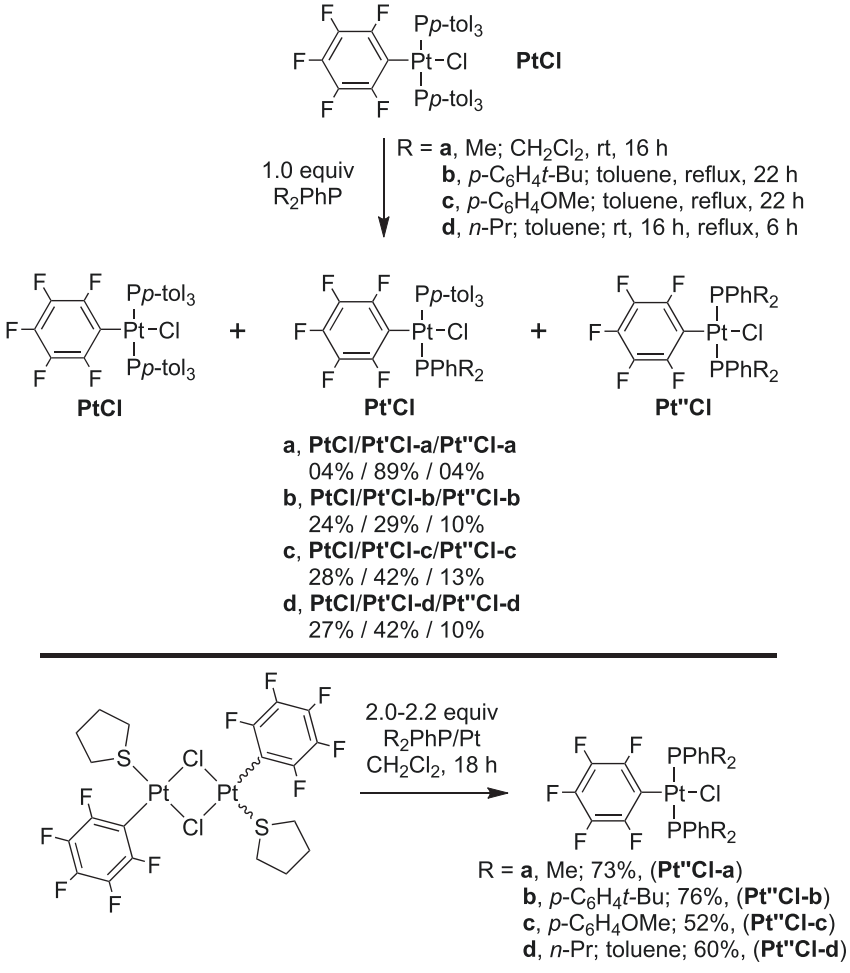

Scheme 2. Syntheses of monoplatinum complexes *trans*-(C_6F_5)(R_2PhP)(*p*-tol_3P)Pt(Cl) (**Pt′Cl**; top) and *trans*-(C_6F_5)(R_2PhP)$_2$Pt(Cl) (**Pt″Cl**; bottom).

CH_2Cl_2. However, after 22 h in refluxing toluene, the target complexes *trans*-(C_6F_5)(*p*-tol_3P)((*p*-*t*-$BuC_6H_4)_2PhP$)Pt(Cl) (**Pt′Cl-b**) and *trans*-(C_6F_5)(*p*-tol_3P)((*p*-$MeOC_6H_4)_2PhP$)Pt(Cl) (**Pt′Cl-c**) could be isolated in 29–42% yields following chromatography.

When **PtCl** and *n*-Pr_2PhP were combined in CH_2Cl_2 or toluene at room temperature, conversion to *trans*-(C_6F_5)(*p*-tol_3P)(*n*-Pr_2PhP)Pt(Cl) (**Pt′Cl-d**) was slow and incomplete. However, the yield of **Pt′Cl-d** improved to 42% when the sample was refluxed in toluene (6 h). In each of these reactions, smaller amounts of the disubstituted byproducts **Pt″Cl-b-d** were also obtained, as verified by independent syntheses (Scheme 2, bottom). Thus, not all of the starting **PtCl** was consumed.

Analogous complexes with the bulkier phosphine *t*-Bu_2PhP were sought, but no reaction took place with **PtCl** in refluxing toluene. Thus, alternative routes were explored as summarized in Scheme 3. First, reactions of [(C_6F_5)(tht)Pt(μ-Cl)]$_2$ and excess *t*-Bu_2PhP in CH_2Cl_2 or refluxing toluene yielded the monophosphine complex (C_6F_5)(*t*-Bu_2PhP)(tht)Pt(Cl) (**1**) instead of the target bis(phosphine) complex *trans*-(C_6F_5)(*t*-$Bu_2PhP)_2$Pt(Cl) (**Pt″Cl-e**; compare to Scheme 2, bottom). The stereochemistry depicted in Scheme 3 was confirmed by a crystal structure (below). Subsequent reactions of **1** with the phosphines Et_3P or *p*-tol_3P in refluxing toluene resulted in *t*-Bu_2PhP displacement. The two-fold substitution products *trans*-(C_6F_5)($Et_3P)_2$Pt(Cl) or *trans*-(C_6F_5)(*p*-$tol_3P)_2$Pt(Cl) (**PtCl**) described earlier [2a,c] were isolated.

Next, the previously reported dichloride complex *trans*-(*t*-$Bu_2PhP)_2Pt(Cl)_2$ (**2**) was synthesized by a slight modification of the literature procedure (Scheme 3, bottom) [12]. The $^1J_{PPt}$ value (2542 Hz) indicated a *trans* stereochemistry [13], in accord with a crystal structure [14]. However, subsequent additions of C_6F_5Li (prepared *in situ* from *n*-BuLi and C_6F_5Br) [15] in either 1:1 or 1:2 stoichiometries gave mainly starting material. Up to 20% conversion to a new species could be observed in some experiments, but the properties were not appropriate for the target molecule.

Finally, routes involving the previously described cyclooctadiene complex (cod)(C_6F_5)Pt(Cl) were investigated (Scheme 3, bottom) [16]. No reaction took place with *t*-Bu_2PhP (2.7 equiv) at room temperature, but *trans*-(C_6F_5)(*t*-$Bu_2PhP)_2$Pt(Cl) (**Pt″Cl-e**) formed cleanly in refluxing toluene. A 64% yield was isolated after workup. A subsequent reaction with *p*-tol_3P (1.0 equiv) in refluxing

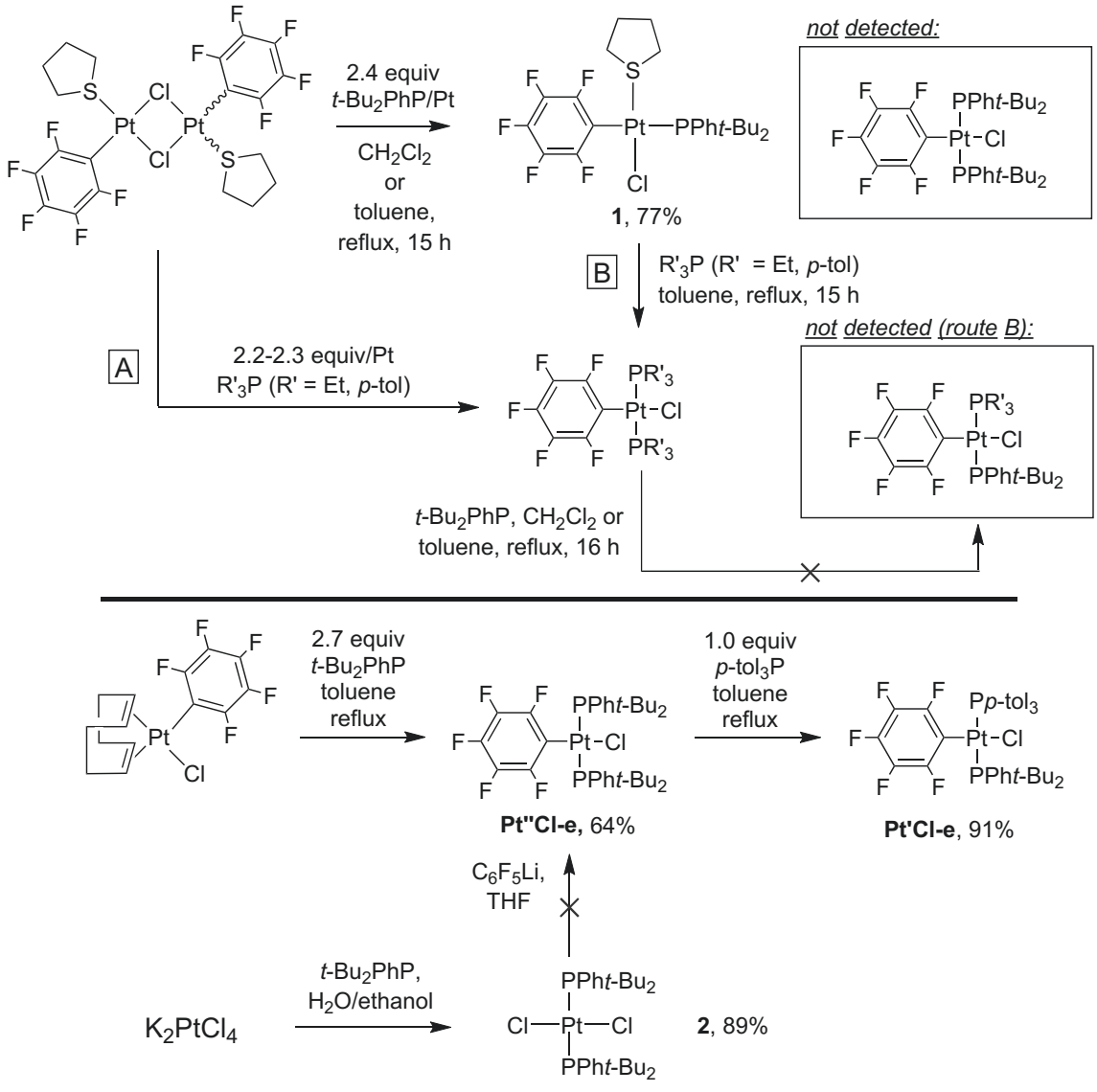

Scheme 3. Successful and unsuccessful routes to the monoplatinum complexes *trans*-(C_6F_5)(*t*-Bu_2PhP)(*p*-tol_3P)Pt(Cl) (**Pt″Cl-e**) and *trans*-(C_6F_5)(*t*-Bu_2PhP)(*p*-tol_3P)Pt(Cl) (**Pt′Cl-e**).

toluene gave the target complex **Pt′Cl-e** in 91% yield.

2.2. Syntheses of butadiynyl complexes trans-(C_6F_5)(R_2PhP)(p-tol_3P)Pt(C≡C)$_2$H (Pt′C_4H)

The next objective was to convert the chloride complexes **Pt′Cl-a-e** to the corresponding butadiynyl complexes. As shown in Scheme 4 (top), conditions that were effective in an earlier synthesis of *trans*-(C_6F_5)(*p*-tol_3P)$_2$Pt(C≡C)$_2$H (**PtC$_4$H**) [2a] were applied to **Pt′Cl-a** (excess butadiyne, $HNEt_2$, cat. CuI). A chromatographic workup gave the target complex *trans*-(C_6F_5)(Me_2PhP)(*p*-tol_3P)Pt(C≡C)$_2$H (**Pt′C$_4$H-a**) in 36% yield, together with lesser amounts of the phosphine scrambling products **PtC$_4$H** (16%) and **Pt″C$_4$H-a** (10%). In an alternative approach, the butadiynyl complex **PtC$_4$H** was treated with Me_2PhP (1.0 equiv, CH_2Cl_2, 18 h). Chromatography gave a comparable product distribution: **Pt′C$_4$H-a**, 30%, **PtC$_4$H**, 18%, **Pt″C$_4$H-a**, 11%.

When the di(*n*-propyl)phenylphosphine chloride complex **Pt′Cl-d** and butadiyne were similarly reacted, NMR analyses showed the formation of a 92:4:4 mixture of the target complex **Pt′C$_4$H-d** and the phosphine scrambling products **PtC$_4$H** and **Pt″C$_4$H-d**. Crystallization afforded pure **Pt′C$_4$H-d** in 73% yield. Interestingly, the two complexes with triarylphosphine ligands, **Pt′Cl-b**,**c**, did not give detectable phosphine scrambling. Workups afforded the butadiynyl complexes **Pt′C$_4$H-b**,**c** in 75–77% yields. As summarized in Scheme 4 (bottom), all attempts to replace the chloride ligand in **Pt′Cl-e** by alkynyl ligands were unsuccessful. Alternative cross coupling protocols (see also below) [2d] involving *t*-BuOK base and KPF_6 gave no reaction.

2.3. Syntheses of diplatinum butadiynediyl complexes

Numerous diplatinum butadiynediyl complexes have been prepared by Hagihara heterocouplings of platinum butadiynyl and platinum chloride complexes [2a,c,d]. Thus, as shown in Scheme 5, equimolar quantities of the butadiynyl complexes **Pt′C$_4$H-a-c** (see Scheme 4) and chloride complexes **Pt′Cl-a-c** (see Scheme 2) were combined in $HNEt_2$ in the presence of a catalytic amount of CuCl. After 66–88 h at 45–50 °C, workups gave mixtures of five to six diplatinum butadiynediyl complexes. Although the individual yields were low, they could be separated by silica gel column chromatography.

It quickly became apparent that the many products were derived from scrambling of the phosphine ligands. In our previous applications of Hagihara coupling reactions, all of the phosphine ligands had been identical, so this phenomenon remained undetected. In accord with nomenclature introduced above, the three possible endgroups could be designated **Pt** ((C_6F_5)(*p*-tol_3P)$_2$Pt), **Pt′** ((C_6F_5)(*p*-tol_3P)(R_2PhP)Pt), and **Pt″** ((C_6F_5)(R_2PhP)$_2$Pt). These can in turn code for the six possible products, **PtC$_4$Pt**, **PtC$_4$Pt′**, **PtC$_4$Pt″**, **Pt′C$_4$Pt′**, **Pt′C$_4$Pt″** and **Pt″C$_4$Pt″**.

In the case where the phenylphosphine substituents (R_2) were Me (**a**), five diplatinum complexes were isolated: **PtC$_4$Pt**, 3%; **PtC$_4$Pt′-a**, 23%; **PtC$_4$Pt″-a**, 12%; **Pt′C$_4$Pt′-a**, 27%; **Pt′C$_4$Pt″-a**, 4%. The

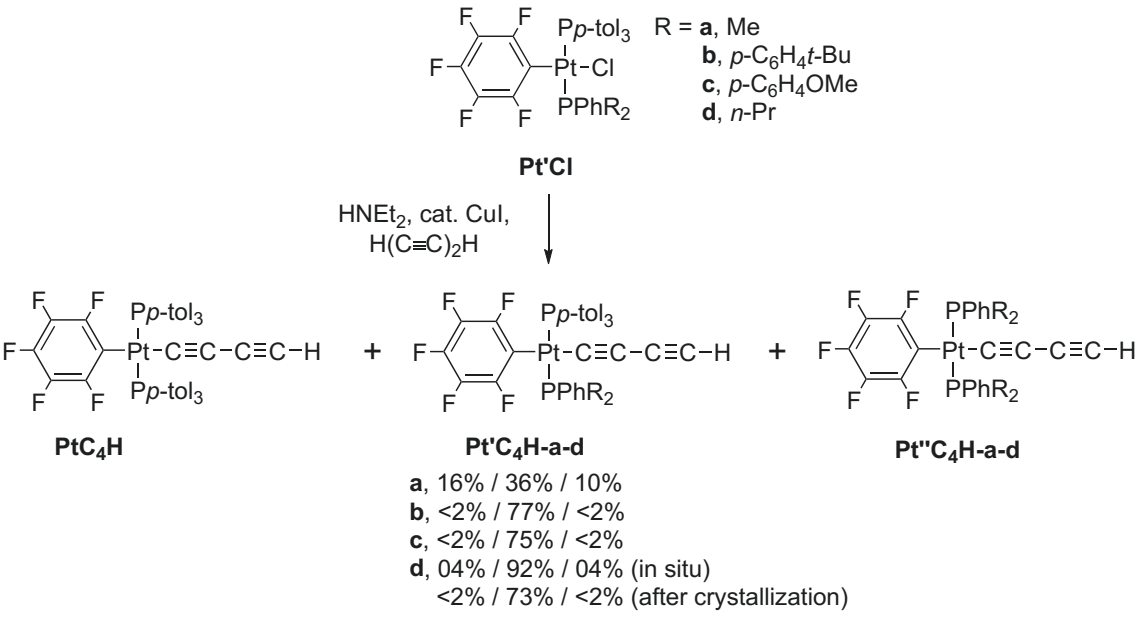

Scheme 4. Successful and unsuccessful syntheses of monoplatinum butadiynyl and alkynyl complexes.

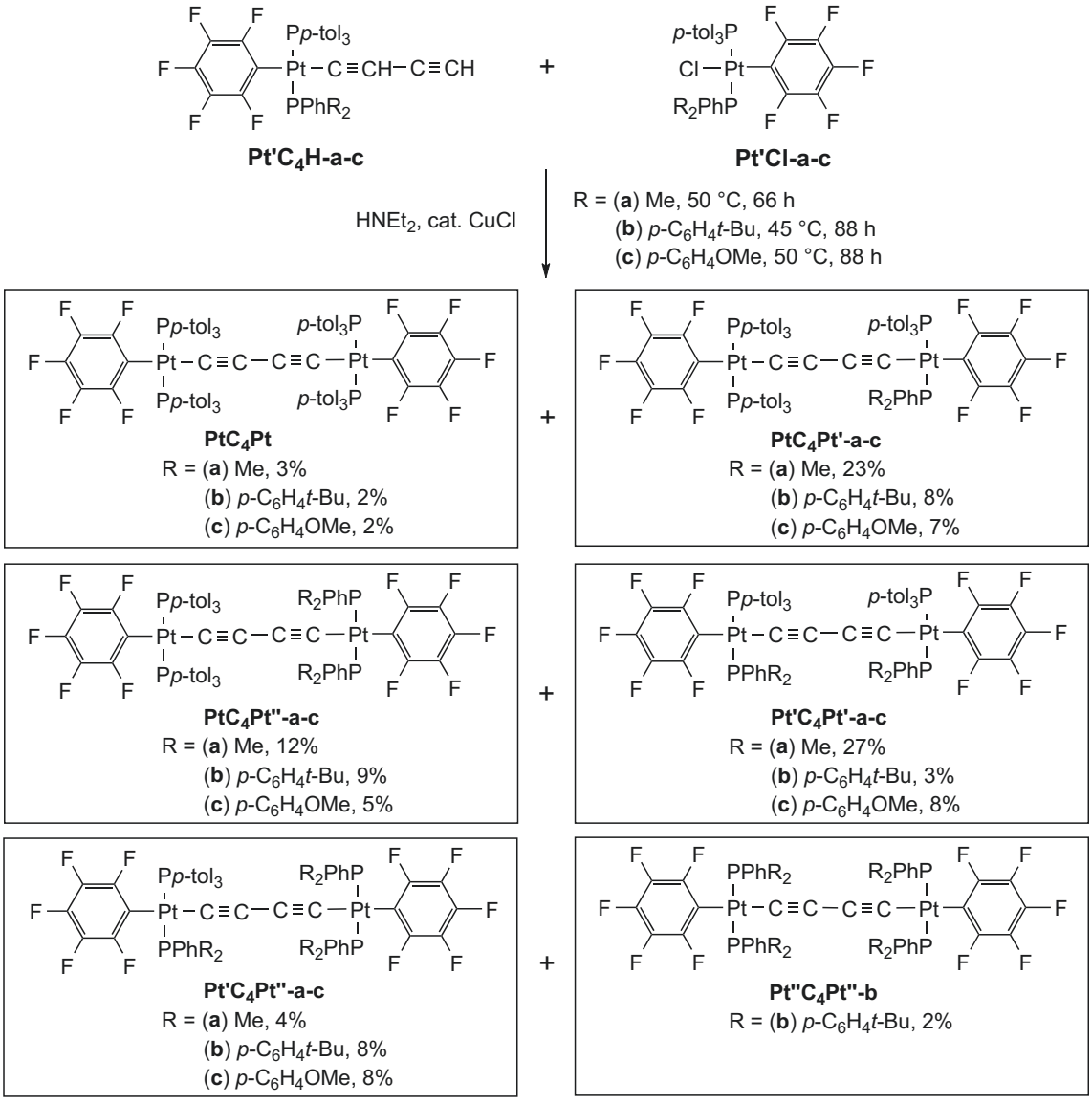

Scheme 5. Syntheses of diplatinum butadiynyl complexes.

R_f values decreased as the number of Me_2PhP ligands increased. All were air stable yellow solids, and were characterized by NMR (^1H, $^{13}C\{^1H\}$, $^{31}P\{^1H\}$) and microanalyses, as summarized in the experimental section. The structures readily followed from the NMR properties, principal details of which are described below.

In the case where the phenylphosphine substituents were *p*-*t*-BuC_6H_4 (**b**), six diplatinum complexes were isolated: **PtC$_4$Pt**, 2%; **PtC$_4$Pt′-b**, 8%; **PtC$_4$Pt″-b**, 9%; **Pt′C$_4$Pt′-b**, 3%; **Pt′C$_4$Pt″-b**, 8%; **Pt″C$_4$Pt″-b**, 2%. In the case where the phenylphosphine substituents were *p*-$MeOC_6H_4$ (**c**), five complexes were isolated as summarized in Scheme 5. This coupling was somewhat slower, so a significant amount of unreacted chloride complex **Pt′Cl-c** (26%) was recovered, together with traces of the scrambled analog **PtCl** (1%).

Given these disappointing results, attention was turned to an alternative recipe for cross coupling metal chloride and terminal alkynyl complexes. It had been shown that when THF/methanol solvent mixtures were employed with slight excesses of *t*-BuOK and KPF_6 and a catalytic amount of CuCl, diplatinum butadiynediyl complexes could be isolated in good yields [2d]. This protocol was optimized using equimolar quantities of the *p*-tol_3P substituted reaction partners *trans*-$(C_6F_5)(p\text{-}tol_3P)_2Pt(C{\equiv}C)_2H$ (**PtC$_4$H**) and **PtCl**. As described elsewhere [17], workup gave the known complex **PtC$_4$Pt** in 73% yield.

Next, comparable conditions were applied to coupling partners that each contained two different phosphine ligands. As shown in Scheme 6, **Pt′C$_4$H-b** and **Pt′Cl-b** were reacted for 15 d at room temperature. Workup gave the target complex **Pt′C$_4$Pt′-b** in 21% yield, as well as traces of **PtC$_4$Pt′-b** and **Pt′C$_4$Pt″-b** (ca. 1% each). Considerable amounts of **Pt′C$_4$H-b** and **Pt′Cl-b** were recovered (19%, 36%). Comparable conversions were realized after 3–4 d at 50 °C. Finally, **Pt′C$_4$H-d** and **Pt′Cl-d** were similarly reacted. Workup after 92 h at room temperature gave the target complex **Pt′C$_4$Pt′-d** in 76% yield after crystallization. No chromatographic purification step was necessary, and no phosphine scrambling byproducts were apparent.

2.4. NMR properties

Certain NMR features of the preceding complexes merit note. In our earlier paper involving similar diplatinum ethynediyl

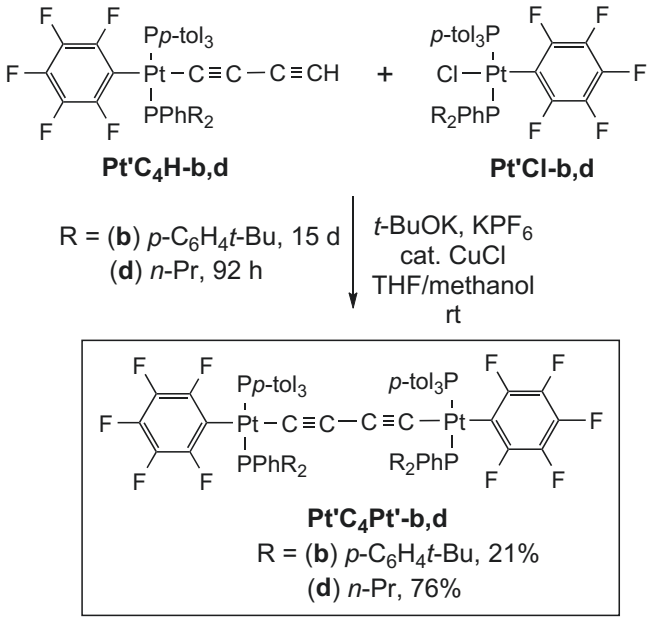

Scheme 6. Syntheses of diplatinum butadiynyl complexes; alternative cross coupling procedure.

complexes [8], no coupling was observed between phosphine ligands on opposite termini (small $^5J_{PP}$). The same would be expected for the more widely separated phosphine ligands in the diplatinum butadiynediyl complexes in this study (still smaller $^7J_{PP}$). Thus, to a first approximation, their NMR spectra should be "hybrids" of those of the monoplatinum butadiynyl complexes corresponding to each endgroup.

This leads to a hierarchy of complexity. First, there are two "series" of butadiynediyl complexes with identical endgroups, each with two *identical* phosphine ligands: **PtC$_4$Pt** (previously reported) and **Pt″C$_4$Pt″-b** (isolated only in trace quantities). These give much simpler spectra. Next, there are the title complexes with identical endgroups, each with two *different* phosphine ligands: **Pt′C$_4$Pt′-a-d**. The ^{1}H NMR spectra exhibit the characteristic signals of each phosphine, with only a few cases of resolved second order phenomena. However, the $^{13}C\{^1H\}$ and $^{31}P\{^1H\}$ NMR spectra exhibit a variety of second order features as described below. Finally, there are three series of complexes with non-identical endgroups: **PtC$_4$Pt′-a-c**, **PtC$_4$Pt″-a-c**, and **Pt′C$_4$Pt″-a-c**. While in theory these give the most complicated NMR spectra, this is only in an additive sense; they seldom introduce new phenomena not manifested in the other complexes.

With regard to the $^{31}P\{^1H\}$ NMR spectra, certain trends in the monoplatinum complexes deserve comment. First, **Pt′Cl-a,d** and **Pt′C$_4$H-a,d** feature one triarylphosphine ligand and one dialkylphenylphosphine ligand. They exhibit well separated signals (δ 18.3 to 20.2, *p*-tol$_3$P; -9.9 to 8.8, R$_2$PPh) and couple as expected ($^2J_{PP}$ = 404–450 Hz). However, **Pt′Cl-b,c** and **Pt′C$_4$H-b,c** feature two similar triarylphosphine ligands [18]. With **Pt′Cl-b** and **Pt′C$_4$H-b**, only one singlet is observed (δ 19.8–17.8), presumably due to accidental degeneracy. With **Pt′Cl-c** and **Pt′C$_4$H-c**, two closely spaced singlets are found (δ 19.51–19.57, 17.58–17.64).

All of these trends extend to the diplatinum butadiynediyl complexes **Pt′C$_4$Pt′-a-d**. However, when $^{31}P\{^1H\}$ NMR spectra of **Pt′C$_4$Pt′-b** were recorded at -80 °C, separate signals for the *p*-tol$_3$P and (*p*-*t*-BuC$_6$H$_4$)$_2$PhP ligands could be observed (δ (CD_2Cl_2) 13.79 and 13.91 as opposed to one signal at 14.00 at 22 °C). Importantly, the structures of all four complexes have been confirmed crystallographically (below).

The $^{13}C\{^1H\}$ NMR spectra of **Pt′Cl-a,d**, **Pt′C$_4$H-a,d**, and **Pt′C$_4$Pt′-a,d** are unexceptional. However, those of **Pt′Cl-b,c**, **Pt′C$_4$H-b,c**, and **Pt′C$_4$Pt′-b,c** are complicated by numerous "virtual couplings" [19]. That of **Pt′C$_4$Pt′-b** features a variety of virtual triplets (typically

Table 1
Summary of crystallographic data for monoplatinum complexes.

Complex	**1**	**Pt′Cl-e**	**Pt′C$_4$H-a**
empirical formula	$C_{48}H_{62}Cl_2F_{10}P_2Pt_2S_2$	$C_{34}H_{46}ClF_5P_2Pt$	$C_{39}H_{33}F_5P_2Pt$
formula weight	1416.12	842.19	853.68
temperature (K)	110(2)	110(2)	110(2)
diffractometer	Bruker D8 GADDS	Bruker Apex 2	Bruker Smart
wavelength (Å)	0.71073	0.71073	0.71073
crystal system	monoclinic	orthorhombic	triclinic
space group	$P2_{1/n}$	$P2_12_12_1$	$P\bar{1}$
unit cell dimensions			
a (Å)	13.403(8)	12.1059(15)	9.502(5)
b (Å)	16.599(10)	14.2630(18)	11.234(5)
c (Å)	24.219(15)	20.214(2)	16.775(8)
α (°)	90	90	82.188(6)
β (°)	102.724(8)	90	83.654(6)
γ (°)	90	90	73.939(6)
Volume (Å^3)	5256(6)	3490.3(7)	1699.8(14)
Z	4	4	2
ρ_{calcd} (Mg•m^{-3})	1.790	1.603	1.668
μ mm^{-1}/F(000)	5.627/2768	4.238/1680	4.277/840
Crystal size mm^3	0.05 × 0.04 × 0.03	0.60 × 0.40 × 0.10	0.35 × 0.15 × 0.15
θ range of data collection (°)	1.50 to 28.76	2.43 to 27.50	1.23 to 27.76
index ranges	$-18 \le h \le 17$	$-15 \le h \le 15$	$-12 \le h \le 12$
	$-22 \le k \le 21$	$-18 \le k \le 18$	$-14 \le k \le 14$
	$-32 \le l \le 32$	$-25 \le l \le 26$	$-21 \le l \le 21$
reflections collected/independent	58195/12840	39178/7918	19785/7793
data/restraints/parameters	12840/123/610	7918/0/400	7793/0/423
goodness of fit on F^2	1.073	1.073	1.012
final R indices I > 2σ(I)	$R1 = 0.0468$,	$R1 = 0.0192$,	$R1 = 0.0359$,
	$wR2 = 0.0999$	$wR2 = 0.0399$	$wR2 = 0.0712$
R indices (all data)	$R1 = 0.0823$,	$R1 = 0.0210$,	$R1 = 0.0452$,
	$wR2 = 0.1155$	$wR2 = 0.0404$	$wR2 = 0.0743$
largest diff. peak and hole (eÅ^{-3})	2.735 and −2.208	0.878 and −0.386	2.250 and −2.234

Table 2
Summary of crystallographic data for diplatinum complexes.

Complex	**Pt′C$_4$Pt′-a**·2CH$_2$Cl$_2$	**Pt′C$_4$Pt′-b**	**Pt′C$_4$Pt′-c**	**Pt′C$_4$Pt′-d**	**PtC$_4$Pt″-b**·C$_7$H$_8$
empirical formula	$C_{76}H_{68}Cl_4F_{10}P_4Pt_2$	$C_{110}H_{104}F_{10}P_4Pt_2$	$C_{99}H_{82}F_{10}O_5P_4Pt_2$	$C_{82}H_{80}F_{10}P_4Pt_2$	$C_{117}H_{112}F_{10}P_4Pt_2$
formula weight	1827.16	2129.99	2055.70	1769.52	2222.13
temperature (K)	110(2)	213(2)	110(2)	110(2)	110(2)
diffractometer	Bruker Apex 2	Bruker Apex 2	Bruker D8 GADDS	Bruker D8 GADDS	Bruker D8 GADDS
wavelength (Å)	0.71073	0.71073	1.54178	1.54178	1.54178
crystal system	monoclinic	monoclinic	triclinic	monoclinic	triclinic
space group	*P*2(1)/c	*P*2(1)/n	*P*-1	*P*2/n	*P*-1
unit cell dimensions					
a (Å)	13.8673(12)	15.376(8)	14.276(2)	15.1018(6)	14.3804(7)
b (Å)	20.4887(18)	31.668(15)	15.175(2)	13.6152(6)	14.8720(7)
c (Å)	14.6707(13)	20.056(10)	20.880(3)	18.0925(9)	24.5452(12)
α (°)	90	90	81.953(7)	90	99.639(3)
β (°)	117.9260(10)	94.529(7)	83.809(8)	96.814(3)	92.688(3)
γ (°)	90	90	72.767(8)	90	100.460(3)
Volume (Å^3)	3682.9(6)	9736(8)	4267.4(11)	3693.8(3)	5073.1(4)
Z	2	4	2	2	2
ρ_{calcd} (Mg m^{-3})	1.648	1.453	1.600	1.591	1.453
μ mm^{-1}/F(000)	4.094/1796	3.003/4280	7.394/2044	8.378/1756	6.225/2234
crystal size mm^3	0.15 × 0.14 × 0.05	0.25 × 0.12 × 0.10	0.10 × 0.09 × 0.03	0.15 × 0.07 × 0.03	0.15 × 0.12 × 0.02
θ range of data collection (°)	2.53 to 28.81	2.06 to 27.50	2.14 to 57.50	3.25 to 61.43	1.83 to 60.00
index ranges	$-18 \le h \le 18$ $-27 \le k \le 26$ $-19 \le l \le 19$	$-19 \le h \le 19$ $-41 \le k \le 41$ $-26 \le l \le 26$	$-15 \le h \le 15$ $-16 \le k \le 16$ $-22 \le l \le 22$	$-17 \le h \le 17$ $-15 \le k \le 15$ $-20 \le l \le 20$	$-15 \le h \le 15$ $-16 \le k \le 16$ $-27 \le l \le 27$
reflections collected/independent	42642/9026	113592/22325	33184/10958	23951/5676	37606/14105
data/restraints/parameters	9026/0/438	22325/12/1120	10958/350/1082	5676/65/442	14105/18/1199
goodness of fit on F^2	1.051	1.031	0.960	1.015	1.042
final R indices I > 2σ(I)	$R1 = 0.0349$, $wR2 = 0.0699$	$R1 = 0.0396$, $wR2 = 0.0889$	$R1 = 0.0595$, $wR2 = 0.1449$	$R1 = 0.0368$, $wR2 = 0.0917$	$R1 = 0.0380$, $wR2 = 0.0916$
R indices (all data)	$R1 = 0.0536$, $wR2 = 0.0755$	$R1 = 0.0705$, $wR2 = 0.0994$	$R1 = 0.1003$, $wR2 = 0.1610$	$R1 = 0.0533$, $wR2 = 0.0982$	$R1 = 0.0565$, $wR2 = 0.0964$
largest diff. peak and hole (eÅ^{-3})	1.278 and −1.128	1.461 and −1.024	1.443 and −1.225	1.072 and −0.978	1.786 and −1.146

5–6 Hz for all aryl carbon atoms that are *o*/*m* to phosphorus). In contrast, that of **Pt′C$_4$Pt′-c** exhibits a corresponding number of doublet of doublets, in which the *J* values are very close to those of the virtual triplets. Other complexes that exhibit a large number of virtual triplets include **Pt″Cl-a** and **Pt″C$_4$H-a** (nearly all Me$_2$PhP ligand ^{13}C NMR signals, and the Me$_2$P ^{1}H NMR signal).

Many NMR spectra were recorded at low temperature in hopes of detecting dynamic processes or separate signals for diastereotopic groups as diagrammed in Scheme 1. All of these were uninformative. For example, the ^{1}H NMR spectra of **Pt′C$_4$Pt′-a** and **Pt′C$_4$Pt′-c** (CD$_2$Cl$_2$) did not show any significant changes when cooled to −80 °C. In the case of **Pt′C$_4$Pt′-b**, some ^{1}H NMR peaks became broader, but no decoalescence phenomena were detected. With **Pt′C$_4$Pt′-b**,**c**, the *ipso* carbon atoms of the (*p*-XC$_6$H$_4$)$_2$P moieties are potentially diastereotopic, but only broadened ^{13}C{^{1}H,^{31}P} signals were observed at -80 °C.

NMR spectra of the more soluble complex **Pt′C$_4$Pt′-d** were recorded in the lower freezing solvent CDFCl$_2$ [21]. Some ^{1}H NMR signals merged as the temperature was lowered, but no decoalescence was apparent at -120 °C. The ^{13}C{^{1}H} NMR spectrum

Table 3
Key interatomic distances (Å) and bond or plane/plane angles (°) in diplatinum complexes.

	Pt′C$_4$Pt′-a·2CH$_2$Cl$_2$	**Pt′C$_4$Pt′-b**	**Pt′C$_4$Pt′-c**	**Pt′C$_4$Pt′-d**	**PtC$_4$Pt″-b**·C$_7$H$_8$
Pt(1)-C(1)	1.990(4)	1.995(4)	1.968(14)	2.021(7)	1.994(7)
C(1)≡C(2)	1.219(5)	1.195(5)	1.267(17)	1.186(9)	1.216(8)
C(2)-C(3)[a]	1.376(7)	1.381(6)	1.37(2)	1.392(13)	1.366(9)
C(3)≡C(4)[a]	1.219(5)	1.215(6)	1.28(2)	1.186(9)	1.238(8)
C(4)-Pt(2)[a]	1.990(4)	1.979(4)	1.909(18)	2.021(7)	1.973(6)
Pt(1)-C$_{ipso}$	2.061(4)	2.071(4)	2.069(12)	2.089(6)	2.074(4)
Pt(2)-C$_{ipso}$[a]	2.061(4)	2.072(4)	2.081(14)	2.089(6)	2.071(6)
Pt(1)-P(1)	2.3101(10)	2.3048(14)	2.309(3)	2.3130(16)	2.2971(15)
Pt(1)-P(2)	2.2932(11)	2.3059(14)	2.318(3)	2.3007(17)	2.2980(15)
Pt(2)-P(3)[a]	2.3101(10)	2.3138(14)	2.295(3)	2.3130(16)	2.3044(15)
Pt(2)-P(4)[a]	2.2932(11)	2.2998(14)	2.299(3)	2.3007(17)	2.2905(15)
Av. C$_{sp}$≡C$_{sp}$	1.219	1.205	1.27	1.186	1.227
Pt···Pt	7.792	7.729	7.764	7.792	7.779
sum of bond lengths, Pt(1) to Pt(2)	7.797	7.765	7.79	7.806	7.787
Pt(1)-C(1)-C(2)	176.8(3)	171.0(4)	175.9(12)	174.0(6)	175.5(5)
C(1)-C(2)-C(3)[a]	178.4(5)	178.0(5)	175.9(14)	177.8(9)	178.4(7)
C(2)-C(3)-C(4)[a]	178.4(5)	175.7(5)	174.0(17)	177.8(9)	178.0(6)
C(3)-C(4)-Pt(2)[a]	176.8(3)	169.6(4)	175.9(12)	174.0(6)	176.3(5)
avg. π stacking[b]	3.603	3.708	3.734	4.098	4.042
(P1-Pt1-P2)Pt2 vs. (P3-Pt2-P4)Pt1[c]	0	44.18	51.30	0	46.07
(C$_{ipso}$-P1-Pt1-P2) vs. (P3-Pt2-P4-C$_{ipso}$)[c]	0	43.67	51.71	0	48.46

[a] To facilitate comparisons, some atoms of **Pt′C$_4$Pt′-a**·2CH$_2$Cl$_2$ and **Pt′C$_4$Pt′-d**, both of which exhibit inversion centers, have been renumbered from those in the cif files.
[b] Distance between the centroids of the C$_6$F$_5$ and aryl rings; average of four values.
[c] Angle between planes defined by these atoms.

showed only broadening, and the $^{31}P\{^{1}H\}$ NMR spectrum was essentially unchanged.

2.5. Structural properties

Crystal structures were sought as a means of confirming structural assignments, and for gauging endgroup/endgroup interactions in the diplatinum complexes. Single crystals of **1**, **Pt″Cl-e**, **Pt′C$_4$H-a**, **Pt′C$_4$Pt′-a-d**, and **PtC$_4$Pt″-b** or solvates thereof were grown, and the structures were determined as outlined in Tables 1–3 and the experimental section. Key metrical parameters are provided in Table 3 and Figs. 1–3. Many other tetraphosphine complexes with ArPt(C≡C)$_m$PtAr linkages have been structurally characterized [2,5a-c,e-l,o-q], and the bond lengths and angles in Table 3 are unexceptional.

The molecular structures are depicted in Figs. 1–8, and additional representations are provided below and in the supplementary material. About half of the lattices contained some type of disorder, which was modeled as detailed in the experimental section. Both **Pt′C$_4$Pt′-a** and **Pt′C$_4$Pt′-d** exhibited centers of inversion at the midpoints of the C$_4$ chains.

For the diplatinum complexes, a measure of the "twist" associated with the square planar endgroups was sought. In one approach, least squares planes were defined using the P-Pt-P linkage on one terminus, and the platinum from the other. For the idealized atropisomers in Scheme 1, the angle defined by these two planes would be 90°. As summarized in Table 3, the angles between the planes in the crystal structures ranged from 0° for the complexes with an inversion center to 44–51° for the others. When planes defined by the P-Pt-P linkages and the ligating C$_6$F$_5$ carbon atom (C$_{ipso}$) were employed, the values were very similar.

In the diplatinum complexes, the pentafluorophenyl ligands on each platinum were always sandwiched between two phosphine derived aryl groups. The average centroid-centroid spacing (π stacking distance) for each molecule is given in Table 3 (3.60–4.10 Å). This phenomenon has been seen in many other diplatinum polyynediyl complexes bearing pentafluorophenyl and two *trans*-triarylphosphine ligands [2a,c,e,5e,g,k,l], and has been attributed to quadrupolar interactions between the fluorinated and non-fluorinated aryl groups [20]. Other structural features are analyzed in the discussion section.

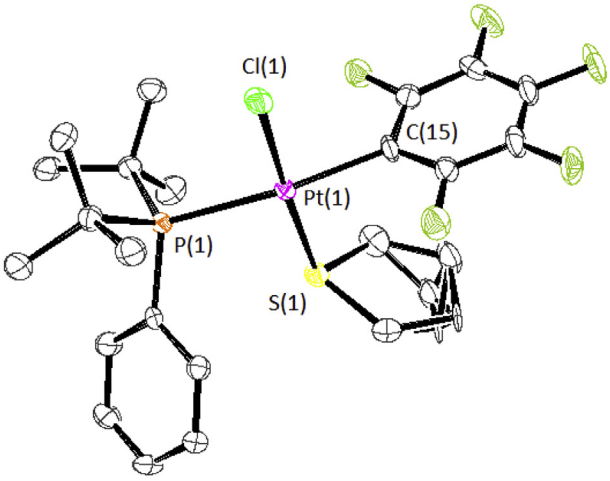

Fig. 1. Molecular structure of **1** with thermal ellipsoids at 50% probability level. Key bond lengths (Å) and angles (°): Pt(1)-C(15), 2.077(8); Pt(1)-S(1), 2.302(2); Pt(1)-Cl(1), 2.342(2); Pt(1)-P(1), 2.365(2); C(15)-Pt(1)-S(1), 90.4(2); C(15)-Pt(1)-Cl(1), 86.5(2); S(1)-Pt(1)-Cl(1), 176.26(7); C(15)-Pt(1)-P(1), 177.9(2); S(1)-Pt(1)-P(1), 88.90(7); Cl(1)-Pt(1)-P(1), 94.35(7).

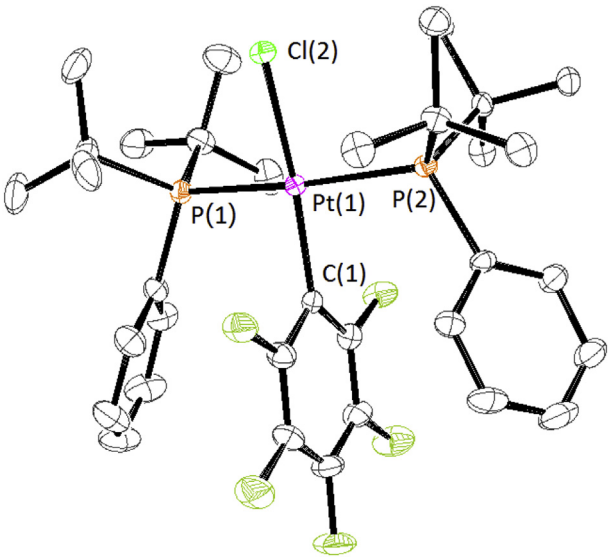

Fig. 2. Molecular structure of **Pt″Cl-e** with thermal ellipsoids at 50% probability level. Key bond lengths (Å) and angles (°): Pt(1)-C(1), 2.020(3); Pt(1)-P(2), 2.3634(8); Pt(1)-P(1), 2.3673(8); Pt(1)-Cl(2), 2.3647(7); C(1)-Pt(1)-P(2), 92.45(8); C(1)-Pt(1)-Cl(2), 168.68(8); P(2)-Pt(1)-Cl(2), 88.52(2); C(1)-Pt(1)-P(1), 90.98(8); P(2)-Pt(1)-P(1), 169.14(3); P(1)-Pt(1)-Cl(2), 90.14(3).

2.6. Other characterization

The UV-visible spectra of diplatinum polyynediyl complexes have been extensively analyzed as a function of carbon chain length [2a,3a,5g]. The λ_{max} red shifts and becomes more intense, and a series of much weaker bands at still longer wavelengths – representing C≡C vibrational fine structure – become increasingly apparent. Such bands were not detected when we initially characterized **PtC$_4$Pt** [2a]. Hence, the UV-visible spectra of representative diplatinum butadiynediyl complexes were recorded at higher

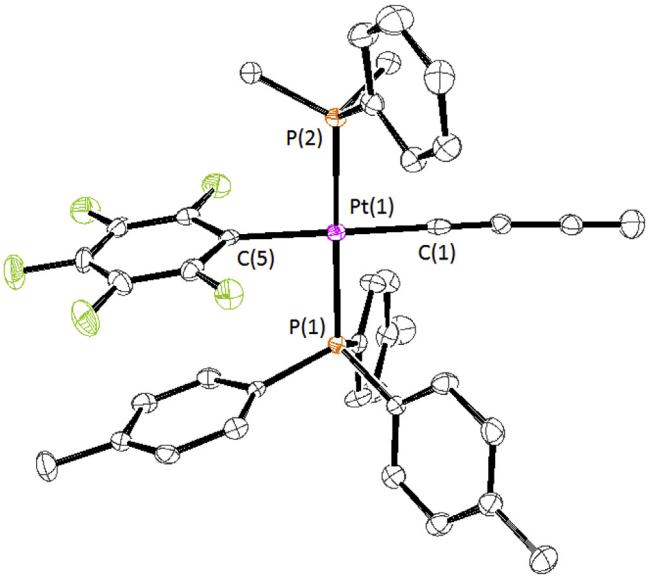

Fig. 3. Molecular structure of **Pt′C$_4$H-a** with thermal ellipsoids at 50% probability level. Key bond lengths (Å) and angles (°): Pt(1)-C(1), 1.993(4); Pt(1)-P(1), 2.3298(13); Pt(1)-P(2), 2.2927(13), Pt(1)-C(5), 2.067(4); C(1)-Pt(1)-P(2), 88.87(11); C(1)-Pt(1)-C(5), 178.05(17); P(2)-Pt(1)-C(5), 91.37(11); C(1)-Pt(1)-P(1), 90.51(11); P(2)-Pt(1)-P(1), 179.30(4); P(1)-Pt(1)-C(5), 89.26(11).

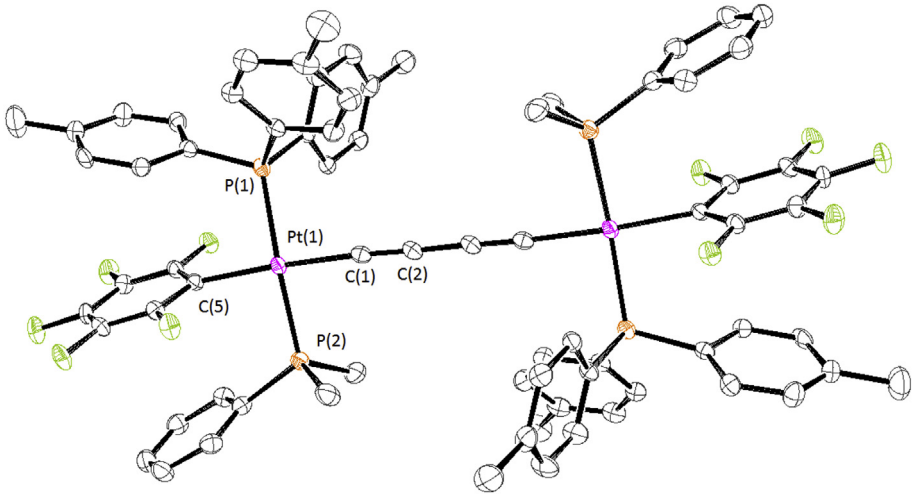

Fig. 4. Molecular structure of **Pt′C$_4$Pt′-a** with thermal ellipsoids at 50% probability level and solvate molecules omitted.

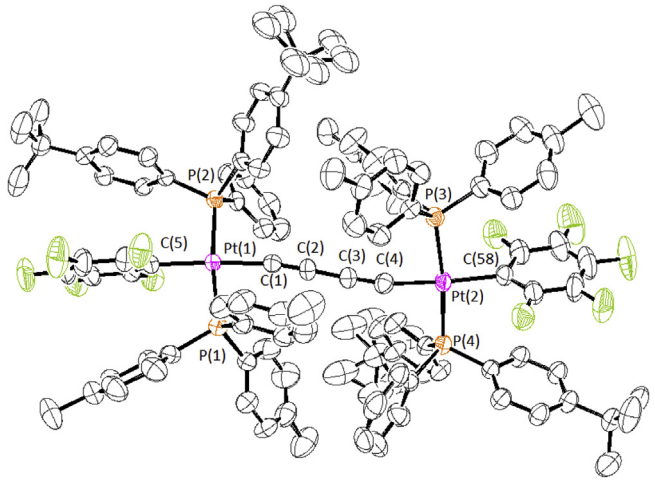

Fig. 5. Molecular structure of **Pt′C$_4$Pt′-b** with thermal ellipsoids at 50% probability level; some *t*-butyl groups are disordered as described in the experimental section.

concentrations and with special attention to this region. As summarized in Table 4, two such bands at 395-387 and 428-422 nm could always be detected. The molar extinction coefficients (ε, $M^{-1}cm^{-1}$) were 500-400 and 120-50, respectively.

3. Discussion

3.1. Syntheses

The preceding data reveal a number of synthetic challenges with respect to both the monoplatinum and diplatinum target complexes. For example, Scheme 3 illustrates the difficulties associated with introducing two bulky *trans* *t*-Bu$_2$PhP ligands onto a C_6F_5PtCl fragment. Although a route to the adduct **Pt″Cl-e** and the substitution product **Pt′Cl-e** could ultimately be realized, several reactions that worked with less bulky phosphine ligands (Scheme 2) were unsuccessful. In the same vein, all efforts to replace the chloride ligand in **Pt′Cl-e** with any type of alkynyl ligand were thwarted (Scheme 4).

The phosphine ligand scrambling that accompanied the

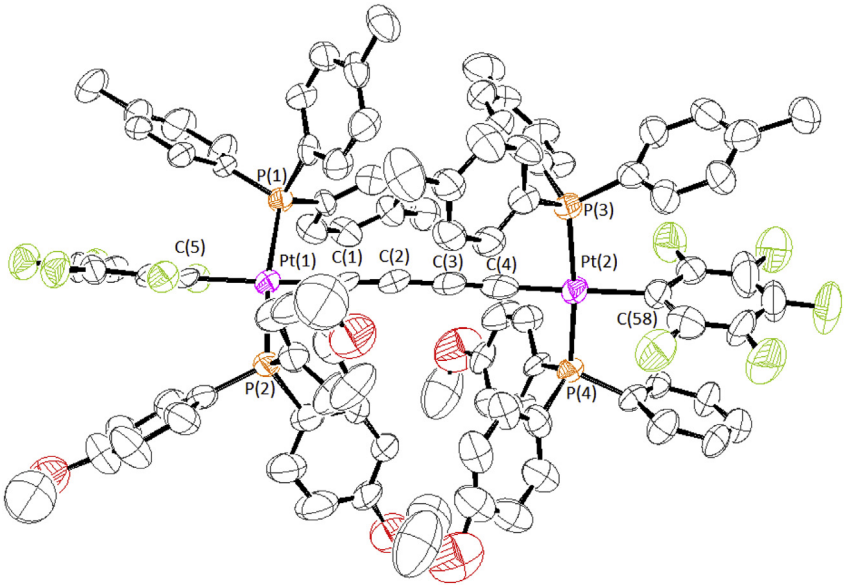

Fig. 6. Molecular structure of **Pt′C$_4$Pt′-c** with thermal ellipsoids at 50% probability level; the methoxy groups are disordered as described in the experimental section.

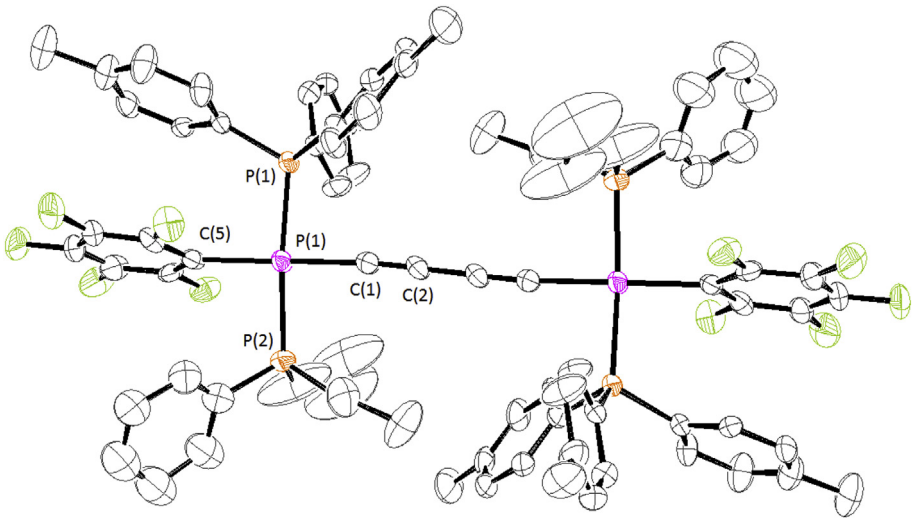

Fig. 7. Molecular structure of **Pt′C$_4$Pt′-d** with thermal ellipsoids at 50% probability level.

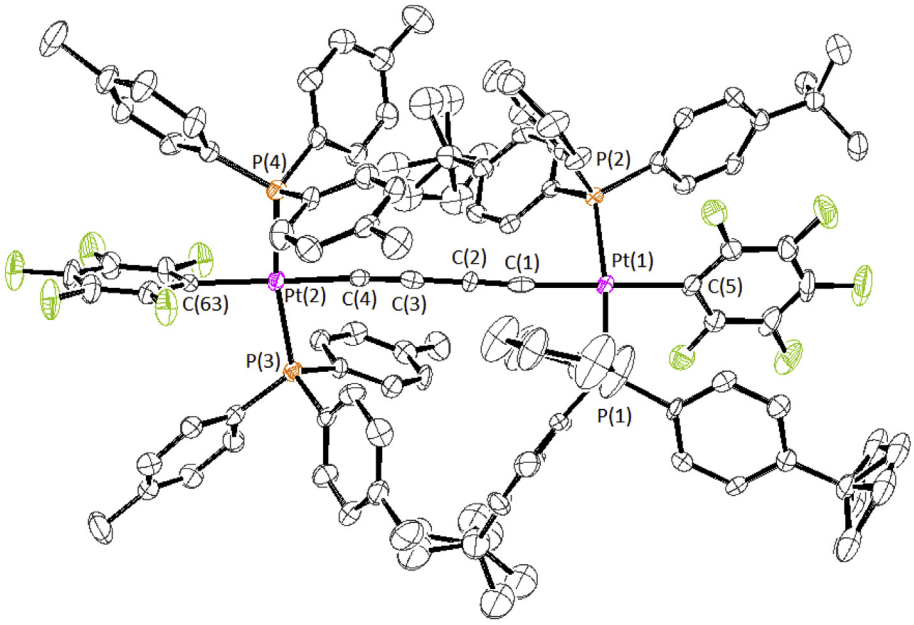

Fig. 8. Molecular structure of **PtC$_4$Pt″-b** with thermal ellipsoids at 50% probability level and solvate molecules omitted; some *t*-butyl groups are disordered as described in the experimental section.

Table 4
UV-visible data for diplatinum butadiynediyl complexes *trans,trans*-(C_6F_5)(*p*-tol_3P)(R_3P)Pt(C≡C)$_2$Pt(PR_3)(P*p*-tol_3)(C_6F_5) in CH_2Cl_2.

Complex	R_3P	λ (nm) [ε ($M^{-1}cm^{-1}$)]
Pt′C$_4$Pt′-a	Me_2PhP	321 [24900], 344 [19500], 388 [560], 422 [79]
Pt′C$_4$Pt′-b	(*p*-*t*-$BuC_6H_4)_2PhP$	293 [16700], 330 [18900], 351 [14700], 393 [470], 427 [80]
Pt′C$_4$Pt′-c	(*p*-$MeOC_6H_4)_2PhP$	311 [12800], 330 [16500], 351 [12600], 392 [470], 427 [120]
Pt′C$_4$Pt′-d	*n*-Pr_2PhP	306 [15000], 322 [20000], 344 [15000], 387 [400], 422 [50]
PtC$_4$Pt	*p*-tol_3P	328 [37000], 351 [12600], 395[500], 428 [90][a]

[a] Reported in reference 2a: 330 [17000], 350 [13200].

coupling of **Pt′C$_4$H-a-c** and **Pt′Cl-a-c** (Scheme 5) was unexpected. This phenomenon was likely masked in earlier studies, which involved reaction components with a single phosphine ligand [2a,c,d]. Enhanced substitution rates are often found with paramagnetic metal complexes [22]. Perhaps the copper catalyst somehow promotes redox equilibria that facilitate scrambling. However, very little or no scrambling is found with the alternative copper catalyzed coupling protocol in Scheme 6. This recipe was not investigated until a late stage of this project. Otherwise, at least some of the target complexes might have been realized in much higher overall yields.

Nonetheless, ligand labilization such as in Scheme 5 can

sometimes be turned into an advantage. For example, one could consider the possibility of carrying out late stage phosphine substitutions simultaneously with coupling. This could greatly increase the breadth of end products accessible, without a corresponding increase in intermediates that must be characterized.

3.2. Structural and dynamic properties

None of the low temperature NMR experiments carried out with the diplatinum butadiynediyl complexes gave any evidence of atropisomerism. Importantly, the many types of NMR couplings observed at ambient temperature (e.g., $^{1}J_{PPt}$, $^{n}J_{HPt}$, $^{n}J_{CPt}$, $^{2}J_{PP}$, certain $^{n}J_{HP}$ and $^{n}J_{CP}$, etc.) exclude the operation of any low energy ligand dissociation processes. These might provide pathways for interconverting atropisomers and/or exchanging diastereotopic groups (see Scheme 1).

This inability to document atropisomerism could have been anticipated if recently published studies with related diplatinum ethynediyl complexes [8] had been carried out first. However, we misjudged the degree of endgroup/endgroup interactions. In this context, Fig. 9 compares space filling representations of three diplatinum complexes: (1) the butadiynediyl complex *trans*,*trans*-$(C_6F_5)(Et_3P)_2Pt(C{\equiv}C)_2Pt(PEt_3)_2(p\text{-tol})$ [2d], which has four identical, moderately sized phosphine ligands, PEt_3, (2) **Pt′C$_4$Pt′-b**, which has bulkier *p*-tol_3P and $(p\text{-}t\text{-}BuC_6H_4)_2PhP$ ligands on each platinum, and (3) the ethynediyl complex *trans*,*trans*-$(C_6F_5)(p\text{-}tol_3P)(Me_2PhP)Pt(C{\equiv}C)Pt(PPhMe_2)(P\text{p-}tol_3)(C_6F_5)$ (**Pt′C$_2$Pt′-a**) [8], which has a smaller Me_2PhP ligand and a bulkier *p*-tol_3P ligand on each platinum. The sp carbon chains are highlighted in dark blue.

In the first complex (Fig. 9, top), the endgroups are well separated and the carbon chain is highly exposed. In the case of **Pt′C$_4$Pt′-b** (Fig. 9, middle), the phosphine ligands on opposite termini have considerable van der Waals contacts, but the carbon chain remains somewhat visible. With this ligand set, the platinum square planes can apparently rotate by 180°, allowing the interconversion of the types of structures in Scheme 1. Concomitant gearing of the aryl groups on the phosphine ligands is required. Space filling representations of all crystallographically characterized complexes are provided in the supplementary material. **Pt′C$_4$Pt′-c** exhibits a slightly higher degree of endgroup/endgroup interactions, but **Pt′C$_4$Pt′-a**,**d** show no van der Waals contacts as all.

The phosphine ligands on opposite termini in **Pt′C$_2$Pt′-a** (Fig. 9, bottom) have extensive van der Waals contacts and nearly completely shield the sp carbon chain. However, low temperature NMR spectroscopy still failed to establish atropisomerism [8], presumably due to a modest barrier to square plane rotation and/or phosphorus substituent gearing. Nonetheless, we consider this a "near miss", as restricted rotation has been observed about other MC_2M' linkages (where one metal is formally octahedral) [23]. Other approaches towards realizing this well established mode of organic stereoisomerism with square planar metal complexes will be pursued in the future. It should also be noted that several other types of atropisomerism have been documented in inorganic and organometallic complexes [24], and conceptually related types of coordination compounds with only axial chirality have been synthesized [25].

3.3. Summary

This study has greatly increased the number of diplatinum butadiynediyl complexes in the literature, particularly with regard to less symmetrically substituted systems. This was assisted by an unanticipated phosphine ligand scrambling process (Scheme 5), which proves avoidable under modified reaction conditions (Scheme 6). These complexes and their precursors exhibit a wealth of fascinating NMR and structural properties. While the diplatinum complexes remain insufficiently congested for any dynamic processes or atropisomerism to be observed, other applications can be anticipated (e.g., improved stabilities of mixed valence Pt(II)/Pt(III) cation radicals) [2a.b.e] and will be investigated in due course.

4. Experimental section

Reactions were conducted under inert atmospheres. Workups were carried out in air. Toluene and CH_2Cl_2 used for reactions were dried and degassed with a Glass Contour solvent purification system; other solvents were used as received from common commercial sources. The following reagents were used as received: CuCl (99.999%, Aldrich), CuI (99.999%, Aldrich), KPF_6 (99.9%, Aldrich), *t*-BuOK (97.0%, TCI), Cl_2PhP (98%, Fluka), Me_2PhP (99%, Strem), *n*-Pr_2PhP (98%, Aldrich), *t*-Bu_2PhP (95%, Aldrich), $(p\text{-}MeOC_6H_4)_2PhP$ (95%, Alfa Aesar), *p*-tol_3P (95%, TCI) and K_2PtCl_4 (99.8%, Aldrich).

NMR spectra were recorded at ambient probe temperature unless noted using a Varian instrument operating at 500.00 (^{1}H), 125.65 (^{13}C{^{1}H}), or 202.28 (^{31}P{^{1}H}) MHz and referenced as follows (δ/ppm): ^{1}H, residual internal $CHCl_3$ (7.26); ^{13}C, internal $CDCl_3$ (77.2); ^{31}P, external H_3PO_4 (0.00). UV/visible spectra were recorded on a Shimadzu UV-1800 spectrophotometer. Melting points were recorded using a Stanford Research Systems (SRS) MPA100 (OptiMelt) automated melting point system. Microanalyses were conducted by Atlantic Microlab.

4.1. *trans*-$(C_6F_5)(Me_2PhP)(p\text{-}tol_3P)Pt(Cl)$ (**Pt′Cl-a**) [11]

A Schlenk flask was charged with *trans*-$(C_6F_5)(p\text{-}tol_3P)_2Pt(Cl)$ (**PtCl** [2a]; 3.170 g, 3.150 mmol), Me_2PhP (0.450 mL, 3.150 mmol) and CH_2Cl_2 (140 mL). The mixture was stirred for 16 h. The solvent was removed by rotary evaporation. The residue was washed with hexane (2 × 20 mL) and dried by oil pump vacuum to give **Pt′Cl-a** as a white powder (2.344 g, 2.790 mmol, 89%), mp 210 °C. Calcd for $C_{35}H_{32}ClF_5P_2Pt$ (840.06): C, 50.04; H, 3.84. Found: 50.01; H, 3.82.

NMR (δ, $CDCl_3$): ^{1}H 7.53 (m, 2H, *o* to P, Ph), 7.47 (dd, $^{3}J_{HH}$ = 9.8 Hz, $^{3}J_{HP}$ = 11.4 Hz, 6H, *o* to P, tol), 7.33 (m, 3H, *m*/*p* to P, Ph), 7.11 (dd, $^{3}J_{HH}$ = 8.1 Hz, $^{4}J_{HP}$ = 1.8 Hz, 6H, *m* to P, tol), 2.35 (s, 9H, CH_3, tol), 1.79 (dd, $^{2}J_{HP}$ = 10.5 Hz, $^{4}J_{HP}$ = 2.7 Hz, $^{3}J_{HPt}$ = 36.9 Hz [29], 6H, PMe_2); ^{13}C{^{1}H} 145.9 (dd, $^{1}J_{CF}$ = 229 Hz, $^{2}J_{CF}$ = 23 Hz, *o* to Pt, C_6F_5), 140.9 (d, $^{4}J_{CP}$ = 2.3 Hz, *p* to P, tol), 136.8 (dm, $^{1}J_{CF}$ = 238 Hz, *m*/*p* to Pt, C_6F_5), 134.5 (d, $^{2}J_{CP}$ = 10.4 Hz, *o* to P, tol), 132.9 (dd, $^{1}J_{CP}$ = 54 Hz, $^{3}J_{CP}$ = 3.1 Hz, *i* to P, Ph), 130.6 (d, $^{2}J_{CP}$ = 9.7 Hz, *o* to P, Ph), 130.3 (d, $^{4}J_{CP}$ = 2.0 Hz, *p* to P, Ph), 128.9 (d, $^{3}J_{CP}$ = 10.8 Hz, *m* to P, tol), 128.4 (d, $^{3}J_{CP}$ = 10.0 Hz, *m* to P, Ph), 126.6 (dd, $^{1}J_{CP}$ = 55.4 Hz, $^{3}J_{CP}$ = 2.7 Hz, $^{2}J_{CPt}$ = 25.8 Hz [29], *i* to P, tol), 111.1 (t, $^{2}J_{CF}$ = 43.5 Hz, *i* to Pt, C_6F_5), 21.5 (s, CH_3, tol), 12.3 (dd, $^{1}J_{CP}$ = 36.6 Hz, $^{3}J_{CP}$ = 1.7 Hz, $^{2}J_{CPt}$ = 37.6 Hz [29], PMe_2); ^{31}P{^{1}H} 20.2 (d, $^{2}J_{PP}$ = 450 Hz, $^{1}J_{PPt}$ = 2624 Hz [29], *p*-tol_3P), −5.5 (d, $^{2}J_{PP}$ = 450 Hz, $^{1}J_{PPt}$ = 2620 Hz [29], PMe_2Ph).

4.2. *trans*-$(C_6F_5)(Me_2PhP)_2Pt(Cl)$ (**Pt″Cl-a**)

A Schlenk flask was charged with $[(C_6F_5)(tht)Pt(\mu\text{-}Cl)]_2$ (1.010 g, 1.040 mmol) [26], Me_2PhP (0.60 mL, 4.20 mmol), and CH_2Cl_2 (70 mL). The solution was stirred for 18 h and filtered through a celite/decolorizing charcoal/glass frit assembly. The solvent was removed by rotary evaporation. The residue was washed with methanol (2 × 20 mL) and dried by oil pump vacuum to give **Pt″Cl-a** as a white powder (0.433 g, 0.643 mmol, 31%). The solvent was removed from the washes by rotary evaporation. The residue was

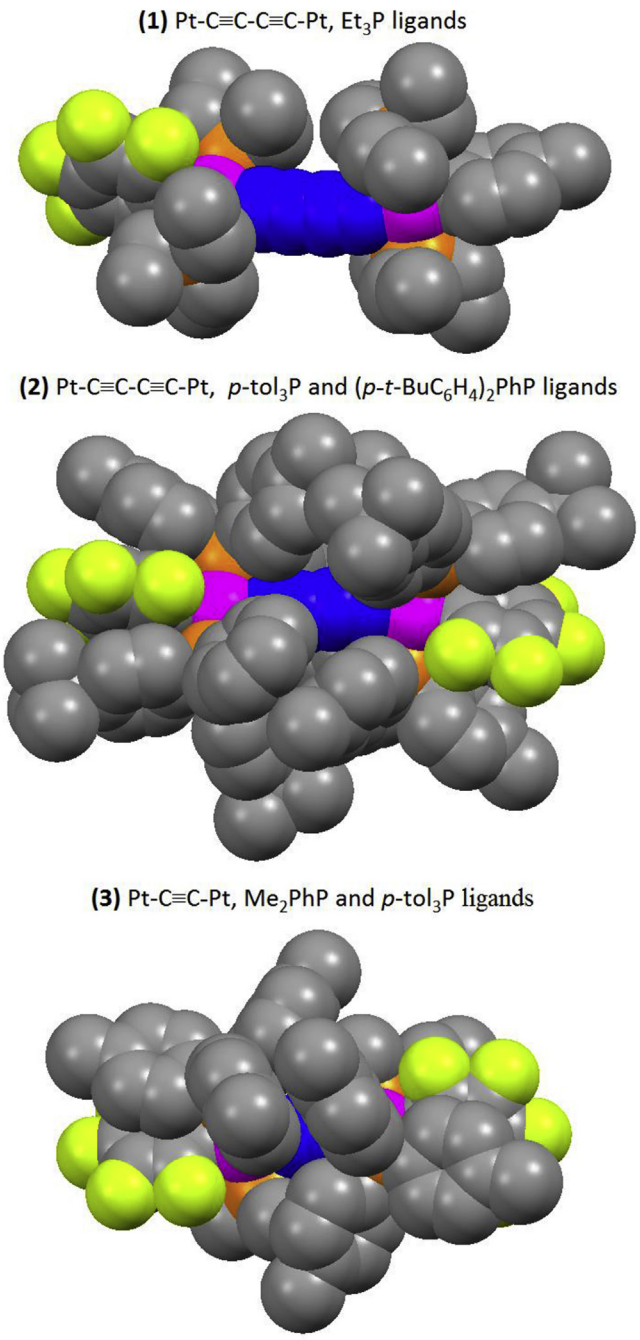

Fig. 9. Representative space filling representations of diplatinum polyynediyl complexes: (1) *trans,trans*-$(C_6F_5)(Et_3P)_2Pt(C{\equiv}C)_2Pt(PEt_3)_2(p\text{-tol})$; (2) **Pt′C$_4$Pt′-b**; (3) *trans,-trans*-$(C_6F_5)(p\text{-tol}_3P)(Me_2PhP)Pt(C{\equiv}C)Pt(PPhMe_2)(P\text{p-tol}_3)(C_6F_5)$ (**Pt′C$_2$Pt′-a**).

recrystallized from methanol/hexane mixture to yield another crop of **Pt″Cl-a** (0.585 g, 0.868 mmol, 42% or 73% total).

NMR (δ, $CDCl_3$): ^{1}H 7.44 (m, 4H, *o* to P), 7.32 (m, 6H, *m*/*p* to P), 1.73 (virtual t [30], $^2J_{HP}$ = 3.9 Hz, $^3J_{HPt}$ = 27.9 Hz [29], 12H, Me); ^{13}C{^{1}H} 146.3 (dd, $^1J_{CF}$ = 228 Hz, $^2J_{CF}$ = 26 Hz, $^2J_{CPt}$ = 76 Hz [29], *o* to Pt, C_6F_5), 136.6 (dm, $^1J_{CF}$ = 247 Hz, *m*/*p* to Pt, C_6F_5), 132.6 (virtual t [30], $^1J_{CP}$ = 28.1 Hz, $^2J_{CPt}$ = 33.2 Hz [29], *i* to P), 130.4 (virtual t [30], $^2J_{CP}$ = 5.8 Hz, *o* to P), 130.3 (s, *p* to P), 128.4 (virtual t [30], $^3J_{CP}$ = 5.1 Hz, *m* to P), 108.1 (t, $^2J_{CF}$ = 43.5 Hz, *i* to Pt, C_6F_5), 12.2 (virtual t [30], $^1J_{CP}$ = 18.9 Hz, $^2J_{CPt}$ = 35.8 Hz [29], PMe_2); ^{31}P{^{1}H} −5.5 (s, $^1J_{PPt}$ = 2520 Hz [29]).

4.3. *trans*-$(C_6F_5)(p\text{-tol}_3P)((p\text{-t-Bu}C_6H_4)_2PhP)Pt(Cl)$ (**Pt′Cl-b**)

A Schlenk flask was charged with **PtCl** (6.186 g, 6.147 mmol) [2a], $(p\text{-t-Bu}C_6H_4)_2PhP$ (2.302 g, 6.147 mmol) [27], and toluene (150 mL). The solution was refluxed for 22 h. The solvent was removed by rotary evaporation and oil pump vacuum. The residue was washed with hexane (3 × 30 mL, leaving 5.213 g) and chromatographed on a silica gel column (3.8 × 42 cm, 8:1 v/v toluene/hexane). The solvent was removed from the product containing fractions by rotary evaporation and oil pump vacuum to give **Pt′Cl-b** (1.906 g, 1.771 mmol, 29%), **PtCl** (1.475 g, 1.466 mmol, 24%), and an unknown complex (0.121 g) as white solids. A fourth fraction contained mainly *trans*-$(C_6F_5)((p\text{-t-Bu}C_6H_4)_2PhP)_2Pt(Cl)$ (**Pt″Cl-b**, ~10%), together with the unknown complex and a second one.

Data for **Pt′Cl-b.** dec pt 249 °C. Calcd. for $C_{53}H_{52}ClF_5P_2Pt$ (1076.46): C 59.14, H 4.87. Found: C 59.31, H 4.86. NMR (δ, $CDCl_3$): ^{1}H 7.88–7.78 (m, 2H, *o* to P, Ph), 7.60–7.47 (m, 10H, *o* to P, tol + C_6H_4), 7.40–7.33 (m, 3H, *m*/*p* to P, Ph), 7.30 (d, $^3J_{HH}$ = 8.4 Hz, 4H, *m* to P, C_6H_4), 7.13 (d, $^3J_{HH}$ = 7.8 Hz, 6H, *m* to P, tol), 2.36 (s, 9H, CH_3, tol), 1.30 (s, 18H, $C(CH_3)_3$); ^{13}C{^{1}H} 153.9 (s, *p* to P, C_6H_4), 145.3 (dd, $^1J_{CF}$ = 225 Hz, $^2J_{CF}$ = 22 Hz, *o* to Pt, C_6F_5), 141.0 (s, *p* to P, tol), 136.3 (dm, $^1J_{CF}$ = 245 Hz, *m*/*p* to Pt, C_6F_5), 135.0 (virtual t [30], $^2J_{CP}$ = 6.3 Hz, *o* to P, Ph), 134.6 (virtual t [30], $^2J_{CP}$ = 6.3 Hz, *o* to P, tol), 134.3 (virtual t [30], $^2J_{CP}$ = 6.3 Hz, *o* to P, C_6H_4), 130.7 (s, *p* to P, Ph), 130.2 (dd, $^1J_{CP}$ = 30.9 Hz, $^3J_{CP}$ = 26.5 Hz, *i* to P, Ph), 128.9 (virtual t [30], $^3J_{CP}$ = 5.7 Hz, *m* to P, tol), 128.2 (virtual t [30], $^3J_{CP}$ = 5.6 Hz, *m* to P, Ph), 126.7 (dd, $^1J_{CP}$ = 31.7 Hz, $^3J_{CP}$ = 27.5 Hz, *i* to P, tol), 126.6 (dd, $^1J_{CP}$ = 31.8 Hz, $^3J_{CP}$ = 27.2 Hz, *i* to P, C_6H_4), 125.1 (virtual t [30], $^3J_{CP}$ = 5.6 Hz, *m* to P, C_6H_4), 114.5 (t, $^2J_{CF}$ = 45.4 Hz, *i* to Pt, C_6F_5), 34.9 (s, $C(CH_3)_3$), 31.2 (s, CH_3); 21.5 (s, CH_3, tol); ^{31}P{^{1}H} 19.8 (s, $^1J_{PPt}$ = 2726 Hz [29]).

4.4. *trans*-$(C_6F_5)((p\text{-t-Bu}C_6H_4)_2PhP)_2Pt(Cl)$ (**Pt″Cl-b**)

A Schlenk flask was charged with $[(C_6F_5)(tht)Pt(\mu\text{-Cl})]_2$ (0.129 g, 0.132 mmol) [26], $(p\text{-t-Bu}C_6H_4)_2PhP$ (0.218 g, 0.582 mmol) [27], and CH_2Cl_2 (20 mL). The solution was stirred for 16 h and filtered through a celite/decolorizing charcoal/glass frit assembly. The solvent was removed by rotary evaporation. The residue was washed with cold methanol (2 × 10 mL) and dried by oil pump vacuum to give **Pt″Cl-b** as a white powder (0.231 g, 0.201 mmol, 76%).

NMR (δ, $CDCl_3$): ^{1}H 7.91–7.80 (m, 4H, *o* to P, Ph), 7.56–7.46 (m, 8H, *o* to P, C_6H_4), 7.44–7.36 (m, 6H, *m*/*p* to P, Ph), 7.28 (d, $^3J_{HH}$ = 8.4 Hz, 8H, *m* to P, C_6H_4), 1.29 (s, 36H, CH_3); ^{31}P{^{1}H} 19.7 (s, $^1J_{PPt}$ = 2731 Hz [29]).

4.5. *trans*-$(C_6F_5)(p\text{-tol}_3P)((p\text{-MeO}C_6H_4)_2PhP)Pt(Cl)$ (**Pt′Cl-c**)

A Schlenk flask was charged with **PtCl** (5.032 g, 5.000 mmol) [2a], $(p\text{-MeO}C_6H_4)_2PhP$ (1.612 g, 5.000 mmol), and toluene (120 mL). The solution was refluxed for 22 h. The solvent was removed by rotary evaporation and oil pump vacuum. The residue was washed with hexane (3 × 50 mL) and chromatographed on a silica gel column (3.8 × 42 cm), using 50:50 v/v CH_2Cl_2/hexane to elute **PtCl**, 80:20 v/v CH_2Cl_2/hexane to elute **Pt′Cl-c**, and 40:60 v/v ethyl acetate/hexane to elute *trans*-$(C_6F_5)((p\text{-MeO}C_6H_4)_2PhP)_2Pt(Cl)$ (**Pt″Cl-c**). The solvent was removed from the fractions by rotary evaporation and oil pump vacuum to give **PtCl** (1.406 g, 1.397 mmol, 28%), **Pt′Cl-c** (2.149 g, 2.098 mmol, 42%) and **Pt″Cl-c** (0.643 g, 0.616 mmol, 13%) as white solids.

Data for **Pt′Cl-c**. mp 215 °C. Calcd for $C_{47}H_{40}ClF_5O_2P_2Pt$ (1024.30): C, 55.11; H, 3.94. Found: 55.06; H, 3.95. NMR (δ, $CDCl_3$): ^{1}H 7.71–7.61 (m, 4H, *o* to P, C_6H_4), 7.59–7.42 (m, 8H, *o* to P, tol + Ph), 7.37–7.29 (m, 1H, *p* to P, Ph), 7.26 (d, $^3J_{HH}$ = 7.2 Hz, 2H, *m* to P, Ph), 7.13 (d, $^3J_{HH}$ = 7.5 Hz, 6H, *m* to P, tol), 6.88 (d, $^3J_{HH}$ = 8.1 Hz, 4H, *m* to

P, C_6H_4), 3.83 (s, 6H, OCH_3), 2.36 (s, 9H, CH_3, tol); $^{13}C\{^1H\}$ 161.5 (s, *p* to P, C_6H_4), 145.2 (dd, $^1J_{CF} = 225$ Hz, $^2J_{CF} = 20$ Hz, *o* to Pt, C_6F_5), 140.9 (s, *p* to P, tol), 136.5 (dm, $^1J_{CF} = 238$ Hz, *m*/*p* to Pt, C_6F_5), 136.4 (virtual t [30], $^2J_{CP} = 6.9$ Hz, *o* to P, C_6H_4), 134.4 (virtual t [30], $^2J_{CP} = 6.3$ Hz, *o* to P, tol), 133.7 (virtual t [30], $^2J_{CP} = 5.9$ Hz, *o* to P, Ph), 131.0 (dd, $^1J_{CP} = 33.9$ Hz, $^3J_{CP} = 23.9$ Hz, *i* to P, Ph), 130.2 (s, *p* to P, Ph), 128.8 (virtual t [30], $^3J_{CP} = 5.5$ Hz, *m* to P, tol), 127.8 (virtual t [30], $^3J_{CP} = 5.2$ Hz, *m* to P, Ph), 126.5 (dd, $^1J_{CP} = 34.4$ Hz, $^3J_{CP} = 24.7$ Hz, *i* to P, tol), 120.5 (dd, $^1J_{CP} = 36.6$ Hz, $^3J_{CP} = 25.9$ Hz, *i* to P, C_6H_4), 114.5 (br, *i* to Pt, C_6F_5), 113.8 (dd, $^3J_{CP} = 6.6$ Hz, $^5J_{CP} = 5.1$ Hz, *m* to P, C_6H_4), 55.4 (s, OCH_3), 21.4 (s, CH_3, tol); $^{31}P\{^1H\}$ 19.565, 19.506 (2 × s, $^1J_{PPt} = 2723$ Hz [29]).

4.6. *trans*-(C_6F_5)((p-$MeOC_6H_4$)$_2$PhP)$_2$Pt(Cl) (**Pt″Cl-c**)

A Schlenk flask was charged with [(C_6F_5)(tht)Pt(μ-Cl)]$_2$ (0.140 g, 0.144 mmol) [26], (p-$MeOC_6H_4$)$_2$PhP (0.210 g, 0.652 mmol), and CH_2Cl_2 (25 mL). The solution was stirred for 16 h and filtered through a celite/decolorizing charcoal/glass frit assembly. The solvent was removed by rotary evaporation. The residue was washed with methanol (2 × 2 mL) and recrystallized from dichloromethane/hexane/methanol to give **Pt″Cl-c** as a white powder (0.155 g, 0.149 mmol, 52%).

NMR (δ, $CDCl_3$): ^1H 7.71–7.60 (m, 8H, *o* to P, C_6H_4), 7.54–7.43 (m, 4H, *o* to P, Ph), 7.38–7.30 (m, 6H, *p* to P, Ph), 7.26 (d, $^3J_{HH} = 7.5$ Hz, 4H, *m* to P, Ph), 6.88 (d, $^3J_{HH} = 8.7$ Hz, 8H, *m* to P, C_6H_4), 3.83 (s, 12H, OCH_3); $^{31}P\{^1H\}$ 19.2 (s, $^1J_{PPt} = 2716$ Hz [29]).

4.7. *trans*-(C_6F_5)(p-tol_3P)(n-Pr_2PhP)Pt(Cl) (**Pt′Cl-d**)

A Schlenk flask was charged with **PtCl** (6.167 g, 6.128 mmol) [2a], n-Pr_2PhP (1.30 mL, 6.190 mmol), and toluene (120 mL). The solution was stirred for 16 h and then refluxed for 6 h. The solvent was removed by rotary evaporation and oil pump vacuum. The residue was washed with hexane (3 × 60 mL). Only unreacted **PtCl** remained (1.096 g, 1.089 mmol, 18%). The solvent was removed from the combined washes by rotary evaporation and oil pump vacuum. The residue was chromatographed on a silica gel column (6.4 × 43 cm) using 50:50 v/v $CHCl_3$/hexane to elute displaced p-tol_3P, 55:45 v/v $CHCl_3$/hexane to elute **Pt″Cl-d**, 60:40 v/v $CHCl_3$/hexane to elute **Pt′Cl-d**, and 80:20 v/v $CHCl_3$/hexane to elute **PtCl**. The solvent was removed from the fractions by rotary evaporation and oil pump vacuum to give **Pt″Cl-d** (0.481 g, 0.612 mmol, 10%), **Pt′Cl-d** (2.295 g, 2.561 mmol, 42%), and **PtCl** (0.511 g, 0.508 mmol, 9% or 27% including the residue isolated above).

Data for **Pt′Cl-d**. NMR (δ, $CDCl_3$): ^1H 7.47 (dd, $^3J_{HP} = 11.0$ Hz, $^3J_{HH} = 8.0$ Hz, 6H, *o* to P, tol; overlapped with m, 2H, *o* to P, Ph), 7.35–7.28 (m, 3H, *m*/*p* to P, Ph), 7.10 (dd, $^3J_{HH} = 8.0$ Hz, $^4J_{HP} = 2.0$ Hz, 6H, *m* to P, tol), 2.35 (s, 9H, CH_3, tol), 2.29–1.95 (m, 4H, PCH_2), 1.79–1.39 (m, 4H, PCH_2CH_2), 1.01 (dt, $^3J_{HH} = 7.5$ Hz, $^4J_{HP} = 0.5$ Hz, 6H, $PCH_2CH_2CH_3$); $^{13}C\{^1H\}$ 145.8 (dd, $^1J_{CF} = 226$ Hz, $^2J_{CF} = 19$ Hz, *o* to Pt, C_6F_5), 140.8 (d, $^4J_{CP} = 2.5$ Hz, *p* to P, tol), 136.6 (dm, $^1J_{CF} = 256$ Hz, *m*/*p* to Pt, C_6F_5), 134.4 (dd, $^2J_{CP} = 11.1$ Hz, $^4J_{CP} = 1.1$ Hz, *o* to P, tol), 131.3 (d, $^2J_{CP} = 8.8$ Hz, *o* to P, Ph), 130.6 (dd, $^1J_{CP} = 50.0$ Hz, $^3J_{CP} = 2.6$ Hz, *i* to P, Ph), 130.0 (d, $^4J_{CP} = 2.4$ Hz, *p* to P, Ph), 128.8 (d, $^3J_{CP} = 10.9$ Hz, *m* to P, tol), 128.2 (d, $^3J_{CP} = 9.8$ Hz, *m* to P, Ph), 126.6 (dd, $^1J_{CP} = 55.0$ Hz, $^3J_{CP} = 3.0$ Hz, *i* to P, tol), 111.1 (t, $^2J_{CF} = 43.8$ Hz, *i* to Pt, C_6F_5), 24.9 (dd, $^1J_{CP} = 32.0$ Hz, $^3J_{CP} = 1.9$ Hz, PCH_2), 21.4 (d, $^5J_{CP} = 1.1$ Hz, CH_3, tol), 17.7 (s, PCH_2CH_2), 15.9 (d, $^3J_{CP} = 14.7$ Hz, $PCH_2CH_2CH_3$); $^{31}P\{^1H\}$ 20.2 (d, $^2J_{PP} = 434$ Hz, $^1J_{PPt} = 2624$ Hz [29], p-tol_3P), 8.8 (d, $^2J_{PP} = 434$ Hz, $^1J_{PPt} = 2629$ Hz [29], n-Pr_2PhP).

4.8. *trans*-(C_6F_5)(n-Pr_2PhP)$_2$Pt(Cl) (**Pt″Cl-d**)

A Schlenk flask was charged with [(C_6F_5)(tht)Pt(μ-Cl)]$_2$ (0.130 g, 0.134 mmol) [26], n-Pr_2PhP (0.13 mL, 0.619 mmol) and CH_2Cl_2 (25 mL). The solution was stirred for 16 h and filtered through a celite/decolorizing charcoal/glass frit assembly. The solvent was removed by rotary evaporation. The residue was recrystallized from hexane to give **Pt″Cl-d** as a white powder (0.125 g, 0.159 mmol, 60%).

NMR (δ, $CDCl_3$): ^1H 7.43–7.37 (m, 4H, *o* to P), 7.29 (d, $^4J_{HP} = 7.0$ Hz, 4H, *m* to P, overlapped with m, 2H, *p* to P), 2.21–1.90 (m, 8H, PCH_2), 1.71–1.33 (m, 8H, PCH_2CH_2), 0.98 (t, $^3J_{HH} = 7.5$ Hz, 12 H, $PCH_2CH_2CH_3$); $^{31}P\{^1H\}$ 8.7 (s, $^1J_{PPt} = 2534$ Hz [29]).

4.9. (C_6F_5)(t-Bu_2PhP)(tht)Pt(Cl) (**1**)

[31] A Schlenk flask was charged with [(C_6F_5)(tht)Pt(μ-Cl)]$_2$ (0.986 g, 1.015 mmol) [26], t-Bu_2PhP (1.16 mL, 4.816 mmol), and CH_2Cl_2 (75 mL). The solution was stirred for 16 h and filtered through a celite/decolorizing charcoal/glass frit assembly. The solvent was removed by rotary evaporation. The residue was washed with cold methanol (2 × 10 mL). Recrystallization from CH_2Cl_2/hexane gave colorless crystals of **1** (1.099 g, 1.552 mmol, 77%).

NMR (δ, $CDCl_3$): ^1H 7.99–7.88 (m, 4H, *o* to P), 7.52–7.43 (d, 6H, *m*/*p* to P), 3.04, 2.71 (each br, 4H, SCH_2), 1.59 (d, 18H, $^3J_{HP} = 13.5$ Hz, $C(CH_3)_3$), 1.42 (br, 4H, SCH_2CH_2); $^{13}C\{^1H\}$ [32] 146.7 (dd, $^1J_{CF} = 222$ Hz, $^2J_{CF} = 22$ Hz, *o* to Pt, C_6F_5), 137.6 (dm, $^1J_{CF} = 243$ Hz, *m*/*p* to Pt, C_6F_5), 135.2 (d, $^2J_{CP} = 8.4$ Hz, *o* to P), 131.2 (d, $^1J_{CP} = 35.3$ Hz, *i* to P), 130.3 (d, $^4J_{CP} = 2.0$ Hz, *p* to P), 127.9 (d, $^3J_{CP} = 8.7$ Hz, *m* to P), 39.4 (s, SCH_2), 37.5 (d, $^1J_{CP} = 18.6$ Hz, $^2J_{CPt} = 17.7$ Hz [29], $C(CH_3)_3$), 30.9 (d, $^2J_{CP} = 3.0$ Hz, CH_3), 29.8 (s, $^3J_{CPt} = 15.9$ Hz [29], SCH_2CH_2); $^{31}P\{^1H\}$ (see Fig. S4) 42.0 (apparent septet, $^4J_{PF} = 34.8$ Hz, $^1J_{PPt} = 2330$ Hz [29]).

4.10. *trans*-(t-Bu_2PhP)$_2$Pt(Cl)$_2$ (**2**) [12,14]

A Schlenk flask was charged with K_2PtCl_4 (1.299 g, 3.130 mmol) and deoxygenated H_2O (10 mL). Another Schlenk flask was charged with t-Bu_2PhP (1.50 mL, 6.295 mmol) and ethanol (10 mL). The ethanol solution was transferred via cannula to the aqueous solution. The resulting pink suspension was stirred. After 1 d, the yellow precipitate was washed with H_2O, ethanol, hexane and diethyl ether, and dried in vacuum to give previously reported **2** (1.968 g, 2.769 mmol, 89%).

NMR (δ, $CDCl_3$): ^1H 7.94 (br, 4H, *o* to P, Ph), 7.42–7.30 (m, 6H, *m*/*p* to P, Ph), 1.61 (virtual t [30], $^3J_{HP} = 6.8$ Hz, 36H, $C(CH_3)_3$); $^{31}P\{^1H\}$ 42.8 (s, $^1J_{PPt} = 2542$ Hz [29]).

4.11. *trans*-(C_6F_5)(t-Bu_2PhP)$_2$Pt(Cl) (**Pt″Cl-e**)

A Schlenk flask was charged with (cod)(C_6F_5)Pt(Cl) (2.797 g, 5.530 mmol) [16], t-Bu_2PhP (3.50 mL, 14.689 mmol) and toluene (120 mL). The solution was refluxed for 48 h. The solvent was removed by rotary evaporation and oil pump vacuum. The residue was washed with ethanol (2 × 25 mL) and hexane (2 × 25 mL) and dried by oil pump vacuum to give **Pt″Cl-e** as a white solid (2.980 g, 3.538 mmol, 64%).

NMR (δ, $CDCl_3$): ^1H 7.90 (br, s, 4H, *o* to P, Ph), 7.24–7.08 (m, 6H, *m*/*p* to P, Ph), 1.58 (t, $^3J_{HP} = 6.0$ Hz, 36H, $C(CH_3)_3$); $^{31}P\{^1H\}$ 41.8 (br s, $^1J_{PPt} = 2668$ Hz).

4.12. *trans*-(C_6F_5)(p-tol_3P)(t-Bu_2PhP)Pt(Cl) (**Pt′Cl-e**)

A Schlenk flask was charged with **Pt″Cl-e** (2.815 g, 3.342 mmol), p-tol_3P (1.025 g, 3.368 mmol) and toluene (120 mL). The solution was refluxed for 14 h. The solvent was removed by rotary evaporation. The residue was washed with methanol (2 × 30 mL), ethanol (20 mL) and hexane (20 mL) to give **Pt′Cl-e** as a white powder

(2.800 g, 3.029 mmol, 91%).

NMR (δ, $CDCl_3$): ^{1}H 7.87–7.80 (m, 2H, *o* to P, Ph), 7.52 (dd, $^3J_{HP}$ = 11.0 Hz, $^3J_{HH}$ = 8.0 Hz, 6H, *o* to P, tol), 7.28–7.21 (m, 3H, *m*/*p* to P, Ph), 7.11 (d, $^3J_{HH}$ = 8.0 Hz, $^4J_{HP}$ = 2.0 Hz, 6H, *m* to P, tol), 2.35 (s, 9H, CH_3, tol) 1.52 (d, $^3J_{HP}$ = 14.0 Hz, 18H, $C(CH_3)_3$); $^{13}C\{^1H\}$ 146.2 (dd, $^1J_{CF}$ = 222 Hz, $^2J_{CF}$ = 20 Hz, *o* to Pt, C_6F_5), 140.8 (d, $^4J_{CP}$ = 2.4 Hz, *p* to P, tol), 136.8 (dm, $^1J_{CF}$ = 254 Hz, *m*/*p* to Pt, C_6F_5), 135.5 (d, $^2J_{CP}$ = 7.9 Hz, *o* to P, Ph), 134.6 (d, $^2J_{CP}$ = 10.7 Hz, *o* to P, tol), 130.1 (d, $^1J_{CP}$ = 38.3 Hz, *i* to P, Ph), 129.6 (d, $^4J_{CP}$ = 1.6 Hz, *p* to P, Ph), 128.7 (d, $^3J_{CP}$ = 11.2 Hz, *m* to P, tol), 126.7 (d, $^3J_{CP}$ = 9.0 Hz, *m* to P, Ph), 126.7 (dd, $^1J_{CP}$ = 58.3 Hz, $^3J_{CP}$ = 1.8 Hz, *i* to P, tol), 111.0 (t, $^2J_{CF}$ = 40.2 Hz, *i* to Pt, C_6F_5), 37.6 (dd, $^1J_{CP}$ = 17.8 Hz, $^3J_{CP}$ = 3.0 Hz, $C(CH_3)$), 31.5 (s, CH_3); 21.5 (s, CH_3, tol); $^{31}P\{^1H\}$ 50.2 (d, $^2J_{PP}$ = 421 Hz, $^1J_{PPt}$ = 2711 Hz [29], *t*-Bu_2PhP), 18.5 (d, $^2J_{PP}$ = 421 Hz, $^1J_{PPt}$ = 2689 Hz [29], *p*-tol_3P).

4.13. *trans*-(C_6F_5)(Me_2PhP)(*p*-tol_3P)Pt(C≡C)$_2$H (**Pt′C$_4$H-a**). Synthesis A

A Schlenk flask was charged with *trans*-(C_6F_5)(*p*-$tol_3P)_2$Pt(C≡C)$_2$H (**PtC$_4$H** [2a]; 0.822 g, 0.806 mmol), Me_2PhP (0.115 mL, 0.811 mmol), and CH_2Cl_2 (60 mL). The solution was stirred for 18 h. The solvent was removed by oil pump vacuum. The residue was washed with hexane (2 × 20 mL). A $^{31}P\{^1H\}$ NMR spectrum of the washes showed signals for *p*-tol_3P, *p*-tol_3PO, and smaller quantities of platinum complexes (~10%). The residue was chromatographed on a silica gel column (2.5 × 30 cm, packed in hexane, eluted with 1:1 v/v CH_2Cl_2/hexane). The solvent was removed from the product containing fractions by rotary evaporation and oil pump vacuum to give **PtC$_4$H** as an off-white solid (0.148 g, 0.145 mmol, 18%), **Pt′C$_4$H-a** as pale yellow solid (0.206 g, 0.242 mmol, 30%), and *trans*-(C_6F_5)($Me_2PhP)_2$Pt(C≡C)$_2$H (**Pt″C$_4$H-a**) as a pale yellow solid (0.061 g, 0.089 mmol, 11%).

Data for **Pt′C$_4$H-a**. mp 128 °C. Calcd for $C_{39}H_{33}F_5P_2Pt$ (853.71): C, 54.87; H, 3.90. Found: 54.66; H, 3.90. NMR (δ, $CDCl_3$): ^{1}H 7.53 (m, 2H, *o* to P, Ph), 7.45 (dd, $^3J_{HH}$ = 8.3 Hz, $^3J_{HP}$ = 11.6 Hz, 6H, *o* to P, tol), 7.35 (m, 3H, *m*/*p* to P, Ph), 7.11 (dd, $^3J_{HH}$ = 7.8 Hz, $^4J_{HP}$ = 1.8 Hz, 6H, *m* to P, tol), 2.36 (s, 9H, CH_3, tol), 1.88 (dd, $^2J_{HP}$ = 10.5 Hz, $^4J_{HP}$ = 2.7 Hz, $^3J_{HPt}$ = 44.4 Hz [29], 6H, PMe_2), 1.69 (t, $^6J_{HP}$ = 1.0 Hz, $^5J_{HPt}$ = 9.3 Hz [29], 1H, ≡CH); $^{13}C\{^1H\}$ 146.4 (dd, $^1J_{CF}$ = 228 Hz, $^2J_{CF}$ = 22 Hz, *o* to Pt, C_6F_5), 140.9 (d, $^4J_{CP}$ = 2.3 Hz, *p* to P, tol), 136.9 (dm, $^1J_{CF}$ = 230 Hz, *m*/*p* to Pt, C_6F_5), 134.4 (d, $^2J_{CP}$ = 10 Hz, $^3J_{CPt}$ = 31 Hz [29], *o* to P, tol), 133.5 (dd, $^1J_{CP}$ = 54.4 Hz, $^3J_{CP}$ = 3.1 Hz, $^2J_{CPt}$ = 28.9 Hz [29], *i* to P, Ph), 130.7 (d, $^2J_{CP}$ = 9.7 Hz, $^3J_{CPt}$ = 28.2 Hz [29], *o* to P, Ph), 130.4 (d, $^4J_{CP}$ = 2.3 Hz, *p* to P, Ph), 128.9 (d, $^3J_{CP}$ = 11.1 Hz, *m* to P, tol), 128.4 (d, $^3J_{CP}$ = 10.4 Hz, *m* to P, Ph), 127.4 (dd, $^1J_{CP}$ = 56.8 Hz, $^3J_{CP}$ = 2.6 Hz, $^2J_{CPt}$ = 27.2 Hz [29], *i* to P, tol), 124.5 (t, $^2J_{CF}$ = 52 Hz, *i* to Pt, C_6F_5), 99.5 (br, $^1J_{CPt}$ = 1011 Hz [29], PtC≡C), 92.7 (s, $^2J_{CPt}$ = 278 Hz [29], PtC≡*C*), 72.4 (t, $^4J_{CP}$ = 2.3 Hz, $^3J_{CPt}$ = 36.7 Hz [29], PtC≡C*C*), 60.1 (s, PtC≡CC≡*C*), 21.5 (s, CH_3, tol), 14.4 (dd, $^1J_{CP}$ = 37.6 Hz, $^3J_{CP}$ = 1.7 Hz, $^2J_{CPt}$ = 45.3 Hz [29], PMe_2); $^{31}P\{^1H\}$ 18.3 (d, $^2J_{PP}$ = 419 Hz, $^1J_{PPt}$ = 2556 Hz [29], *p*-tol_3P), −9.9 (d, $^2J_{PP}$ = 419 Hz, $^1J_{PPt}$ = 2529 Hz [29], Me_2PhP).

Data for **Pt″C$_4$H-a.** NMR (δ, $CDCl_3$): ^{1}H 7.44 (m, 4H, *o* to P, Ph), 7.34 (t, $^3J_{HP}$ = 0.9 Hz, 4H, *m* to P, Ph), 7.32 (m, 2H, *p* to P, Ph), 1.82 (virtual t [30], $^2J_{HP}$ = 3.9 Hz, $^3J_{HPt}$ = 33 Hz [29], 12H, PMe_2; ≡CH signal not observed); $^{13}C\{^1H\}$ [32] 146.7 (dd, $^1J_{CF}$ = 216 Hz, $^2J_{CF}$ = 28 Hz, *o* to Pt, C_6F_5), 136.8 (dm, $^1J_{CF}$ = 258 Hz, *m*/*p* to Pt, C_6F_5), 133.2 (virtual t [30], $^1J_{CP}$ = 28.6 Hz, *i* to P), 130.6 (virtual t [30], $^2J_{CP}$ = 5.8 Hz, *o* to P), 130.4 (s, *p* to P), 128.5 (virtual t [30], $^3J_{CP}$ = 5.1 Hz, *m* to P), 100.2 (br, PtC≡C), 90.3 (s, $^2J_{CPt}$ = 256 Hz [29], PtC≡*C*), 72.2 (s, PtC≡C*C*), 60.2 (s, PtC≡CC≡*C*), 14.3 (virtual t [30], $^1J_{CP}$ = 19.8 Hz, $^2J_{CPt}$ = 44.3 Hz [29], PMe_2); $^{31}P\{^1H\}$ −9.9 (s, $^1J_{PPt}$ = 2426 Hz [29]).

4.14. Synthesis B

A Schlenk flask was charged with **Pt′Cl-a** (0.791 g, 0.942 mmol), CuI (0.040 g, 0.21 mmol), CH_2Cl_2 (6 mL), and $HNEt_2$ (50 mL), and cooled to −45 °C (CO_2/CH_3CN). Then butadiyne (1.7 M in THF, 10.5 mL, 17.5 mmol) [28] was added with stirring. The cold bath was allowed to warm to room temperature (ca. 3 h). After an additional 16 h, the solvent was removed by oil pump vacuum. The residue was extracted with toluene (3 × 20 mL). The combined extracts were filtered through a neutral alumina column (7 cm, packed in toluene). The solvent was removed by rotary evaporation and oil pump vacuum. The residue was washed with ethanol (20 mL) and dried by oil pump vacuum (total mass 0.5015 g). Analysis by $^{31}P\{^1H\}$ NMR established the following product quantities: **Pt′C$_4$H-a** (0.2835 g, 0.332 mmol, 36%), **PtC$_4$H** (0.154 g, 0.151 mmol, 16%), **Pt″C$_4$H-a** (0.064 g, 0.093 mmol, 10%).

4.15. *trans*-(C_6F_5)(*p*-tol_3P)((*p*-*t*-$BuC_6H_4)_2$PhP)Pt(C≡C)$_2$H (**Pt′C$_4$H-b**)

A Schlenk flask was charged with **Pt′Cl-b** (0.539 g, 0.501 mmol), CuI (0.020 g, 0.11 mmol), CH_2Cl_2 (4 mL) and $HNEt_2$ (40 mL), and cooled to −45 °C (CO_2/CH_3CN). Then butadiyne (2.14 M in THF, 4.2 mL, 9.0 mmol) [28] was added with stirring. The cold bath was allowed to warm to 10 °C (ca. 6 h). The cold bath was removed, and after an additional 1 h, the solvent was removed by oil pump vacuum. The residue was extracted with toluene (3 × 25 mL). The combined extracts were filtered through a neutral alumina column (2.5 × 7 cm, packed in toluene). The solvent was removed by rotary evaporation to give **Pt′C$_4$H-b** as an off-white solid (0.418 g, 0.384 mmol, 77%), dec pt 149 °C. Calcd for $C_{57}H_{53}F_5P_2Pt\cdot(CH_2Cl_2)$ (1175.03): C, 59.29; H, 4.72. Found: 59.16; H, 4.72.

NMR (δ, $CDCl_3$): ^{1}H 7.85–7.73 (m, 2H, *o* to P, Ph), 7.62–7.41 (m, 10H, *o* to P, tol + C_6H_4), 7.43–7.34 (m, 3H, *m*/*p* to P, Ph), 7.29 (d, $^3J_{HH}$ = 8.4 Hz, 4H, *m* to P, C_6H_4), 7.12 (d, $^3J_{HH}$ = 7.8 Hz, 6H, *m* to P, tol), 5.31 (s, 2H, CH_2Cl_2), 2.35 (s, 9H, CH_3, tol), 1.47 (t, $^6J_{HP}$ = 0.9 Hz, 1H, ≡CH); 1.29 (s, 18H, $C(CH_3)_3$); $^{13}C\{^1H\}$ 154.0 (s, *p* to P, C_6H_4), 146.0 (dd, $^1J_{CF}$ = 226 Hz, $^2J_{CF}$ = 23 Hz, *o* to Pt, C_6F_5), 141.0 (s, *p* to P, tol), 136.5 (dm, $^1J_{CF}$ = 254 Hz, *m*/*p* to Pt, C_6F_5), 134.9 (virtual t [30], $^2J_{CP}$ = 6.4 Hz, *o* to P, Ph), 134.6 (virtual t [30], $^2J_{CP}$ = 6.4 Hz, *o* to P, tol), 134.3 (virtual t [30], $^2J_{CP}$ = 6.4 Hz, *o* to P, C_6H_4), 131.1 (virtual t [30], $^1J_{CP}$ = 29.3 Hz, *i* to P, Ph), 130.7 (s, *p* to P, Ph), 128.9 (virtual t [30], $^3J_{CP}$ = 5.6 Hz, *m* to P, tol), 128.2 (virtual t [30], $^3J_{CP}$ = 5.5 Hz, *m* to P, Ph), 127.5 (virtual t [30], $^1J_{CP}$ = 30.2 Hz, *i* to P, tol), 127.2 (virtual t [30], $^1J_{CP}$ = 30.0 Hz, *i* to P, C_6H_4), 125.1 (virtual t [30], $^3J_{CP}$ = 5.5 Hz, *m* to P, C_6H_4), 98.1 (s, $^1J_{CPt}$ = 993 Hz [29], PtC≡C), 95.3 (s, $^2J_{CPt}$ = 265 Hz [29], PtC≡*C*), 72.7 (t, $^4J_{CP}$ = 2.5 Hz, $^3J_{CPt}$ = 36.2 Hz [29], PtC≡C*C*), 59.9 (s, PtC≡CC≡*C*), 53.7 (s, CH_2Cl_2), 34.9 (s, $C(CH_3)_3$), 31.3 (s, CH_3); 21.5 (s, CH_3, tol); $^{31}P\{^1H\}$ 17.8 (s, $^1J_{PPt}$ = 2656 Hz [29]).

4.16. *trans*-(C_6F_5)(*p*-tol_3P)((*p*-$MeOC_6H_4)_2$PhP)Pt(C≡C)$_2$H (**Pt′C$_4$H-c**)

Complex **Pt′Cl-c** (1.317 g, 1.286 mmol), CuI (0.051 g, 0.268 mmol), CH_2Cl_2 (10 mL), $HNEt_2$ (80 mL), and butadiyne (2.14 M in THF, 15 mL, 32.1 mmol) [28] were combined in a procedure analogous to that for **Pt′C$_4$H-b**. A similar workup (toluene extraction 3 × 40 mL) gave **Pt′C$_4$H-c** as an off-white solid (0.999 g, 0.962 mmol, 75%), mp 138 °C. Calcd for $C_{51}H_{41}F_5O_2P_2Pt$ (1037.92): C, 59.02; H, 3.98. Found: 58.93; H, 3.98.

NMR (δ, $CDCl_3$): ^{1}H 7.66–7.56 (m, 4H, *o* to P, C_6H_4), 7.55–7.41 (m, 8H, *o* to P, tol + Ph), 7.36–7.29 (m, 1H, *p* to P, Ph), 7.26 (d, $^3J_{HH}$ = 5.4 Hz, 2H, *m* to P, Ph), 7.12 (d, $^3J_{HH}$ = 7.5 Hz, 6H, *m* to P, tol), 6.87 (d, $^3J_{HH}$ = 9.0 Hz, 4H, *m* to P, C_6H_4), 3.84 (s, 6H, OCH_3), 2.36 (s, 9H, CH_3, tol), 1.49 (t, $^6J_{HP}$ = 0.9 Hz, 1H, ≡CH); $^{13}C\{^1H\}$ 161.6 (s, *p* to P, C_6H_4), 145.9 (dd, $^1J_{CF}$ = 225 Hz, $^2J_{CF}$ = 24 Hz, *o* to Pt, C_6F_5), 140.9 (s, *p*

to P, tol), 136.7 (dm, $^{1}J_{CF}$ = 238 Hz, *m*/*p* to Pt, C_6F_5), 136.4 (dd, $^{2}J_{CP}$ = 7.9 Hz, $^{4}J_{CP}$ = 6.3 Hz, *o* to P, C_6H_4), 134.4 (dd, $^{2}J_{CP}$ = 7.0 Hz, $^{4}J_{CP}$ = 5.8 Hz, *o* to P, tol), 133.8 (dd, $^{2}J_{CP}$ = 6.7 Hz, $^{4}J_{CP}$ = 5.5 Hz, *o* to P, Ph), 131.8 (dd, $^{1}J_{CP}$ = 34.4 Hz, $^{3}J_{CP}$ = 24.5 Hz, *i* to P, Ph), 130.3 (s, *p* to P, Ph), 128.8 (dd, $^{3}J_{CP}$ = 6.6 Hz, $^{5}J_{CP}$ = 4.6 Hz, *m* to P, tol), 127.9 (dd, $^{3}J_{CP}$ = 6.2 Hz, $^{5}J_{CP}$ = 4.4 Hz, *m* to P, Ph), 127.4 (dd, $^{1}J_{CP}$ = 35.1 Hz, $^{3}J_{CP}$ = 25.3 Hz, $^{2}J_{CPt}$ = 26.4 Hz [29], *i* to P, tol), 121.4 (dd, $^{1}J_{CP}$ = 37.2 Hz, $^{3}J_{CP}$ = 26.4 Hz, $^{2}J_{CPt}$ = 27.9 Hz [29], *i* to P, C_6H_4), 113.8 (dd, $^{3}J_{CP}$ = 6.9 Hz, $^{5}J_{CP}$ = 5.0 Hz, *m* to P, C_6H_4), 98.0 (s, $^{1}J_{CPt}$ = 989 Hz [29], PtC≡C), 95.2 (s, $^{2}J_{CPt}$ = 267 Hz [29], PtC≡*C*), 72.6 (t, $^{4}J_{CP}$ = 2.5 Hz, $^{3}J_{CPt}$ = 34.5 Hz [29], PtC≡C*C*), 60.1 (s, PtC≡CC≡*C*), 55.4 (s, OCH_3), 21.5 (s, CH_3, tol); $^{31}P\{^{1}H\}$ 17.64, 17.58 (2 × s, $^{1}J_{PPt}$ = 2647 Hz [29]).

4.17. *trans*-(C_6F_5)(*p*-tol$_3$P)(*n*-Pr$_2$PhP)Pt(C≡C)$_2$H (***Pt′C$_4$H-d***)

Complex **Pt′Cl-d** (1.214 g, 1.355 mmol), CuI (0.053 g, 0.278 mmol), CH_2Cl_2 (10 mL), $HNEt_2$ (90 mL), and butadiyne (3.98 M in THF, 6.1 mL, 24.4 mmol) [28] were combined in a procedure analogous to that for **Pt′C$_4$H-c**. A similar workup gave a residue that was recrystallized from hexane to give **Pt′C$_4$H-d** as an off-white solid (0.898 g, 0.987 mmol, 73%), mp 54 °C. Calcd for $C_{43}H_{41}F_5P_2Pt$ (909.81): C, 56.77; H, 4.54. Found: 56.52; H, 4.64.

NMR (*δ*, $CDCl_3$): ^{1}H 7.53–7.47 (m, 2H, *o* to P, Ph), 7.44 (dd, $^{3}J_{HP}$ = 11.0 Hz, $^{3}J_{HH}$ = 8.0 Hz, 6H, *o* to P, tol), 7.37–7.30 (m, 3H, *m*/*p* to P, Ph), 7.10 (dd, $^{3}J_{HH}$ = 8.0 Hz, $^{4}J_{HP}$ = 2.0 Hz, 6H, *m* to P, tol), 2.35 (s, 9H, CH_3, tol), 2.31–2.08 (m, 4H, PCH_2), 1.65 (t, $^{6}J_{HP}$ = 1.0 Hz, 1H, ≡CH), 1.76–1.62, 1.53–1.39 (2 × m, 2H/2H, PCH_2CH_2), 1.02 (dt, $^{3}J_{HH}$ = 7.3 Hz, $^{4}J_{HP}$ = 1.0 Hz, 6H, $PCH_2CH_2CH_3$); $^{13}C\{^{1}H\}$ 146.5 (dd, $^{1}J_{CF}$ = 224 Hz, $^{2}J_{CF}$ = 23 Hz, *o* to Pt, C_6F_5), 140.9 (d, $^{4}J_{CP}$ = 2.4 Hz, *p* to P, tol), 136.9 (dm, $^{1}J_{CF}$ = 248 Hz, *m*/*p* to Pt, C_6F_5), 134.4 (dd, $^{2}J_{CP}$ = 11.3 Hz, $^{4}J_{CP}$ = 1.1 Hz, $^{3}J_{CPt}$ = 20.1 Hz [29], *o* to P, tol), 131.5 (d, $^{2}J_{CP}$ = 9.4 Hz, $^{3}J_{CPt}$ = 17.8 Hz [29], *o* to P, Ph), 131.3 (dd, $^{1}J_{CP}$ = 51.6 Hz, $^{3}J_{CP}$ = 2.6 Hz, *i* to P, Ph), 130.2 (d, $^{4}J_{CP}$ = 2.3 Hz, *p* to P, Ph), 128.8 (d, $^{3}J_{CP}$ = 11.1 Hz, *m* to P, tol), 128.2 (d, $^{3}J_{CP}$ = 9.9 Hz, *m* to P, Ph), 127.5 (dd, $^{1}J_{CP}$ = 56.4 Hz, $^{3}J_{CP}$ = 2.9 Hz, $^{3}J_{CPt}$ = 26.4 Hz [29], *i* to P, tol), 124.4 (t, $^{2}J_{CF}$ = 53 Hz, *i* to Pt, C_6F_5), 98.6 (br, $^{1}J_{CPt}$ = 1000 Hz [29], PtC≡C), 92.7 (s, $^{2}J_{CPt}$ = 274 Hz [29], PtC≡*C*), 72.6 (t, $^{4}J_{CP}$ = 2.4 Hz, $^{3}J_{CPt}$ = 34.9 Hz [29], PtC≡CC), 59.9 (s, PtC≡CC≡*C*), 27.0 (dd, $^{1}J_{CP}$ = 33.3 Hz, $^{3}J_{CP}$ = 1.8 Hz, $^{2}J_{CPt}$ = 33.5 Hz [29], PCH_2), 21.5 (d, $^{5}J_{CP}$ = 1.3 Hz, CH_3, tol), 18.0 (s, $^{3}J_{CPt}$ = 23.5 Hz [29], PCH_2CH_2), 16.1 (d, $^{3}J_{CP}$ = 15.0 Hz, $PCH_2CH_2CH_3$); $^{31}P\{^{1}H\}$ 18.5 (d, $^{2}J_{PP}$ = 404 Hz, $^{1}J_{PPt}$ = 2556 Hz [29], *p*-tol$_3$P), 6.0 (d, $^{2}J_{PP}$ = 404 Hz, $^{1}J_{PPt}$ = 2546 Hz [29], *n*-Pr$_2$PhP).

4.18. *trans,trans*-(C_6F_5)(*p*-tol$_3$P)(Me$_2$PhP)Pt(C≡C)$_2$Pt(PPhMe$_2$)(*p*-tol$_3$)(C_6F_5) (***Pt′C$_4$Pt′-a***)

A Schlenk flask was charged with **Pt′Cl-a** (0.354 g, 0.421 mmol), **Pt′C$_4$H-a** (0.359 g, 0.420 mmol), CuCl (0.016 g, 0.166 mmol), and $HNEt_2$ (60 mL). The mixture was stirred for 65 h at 50 °C. After cooling, the solvent was removed by oil pump vacuum, and the residue extracted with toluene (3 × 20 mL). The combined extracts were filtered through a neutral alumina column (8 cm, packed in toluene). The solvent was removed by rotary evaporation. The residue was chromatographed on a silica gel column (2.5 × 40 cm, 40:60 v/v CH_2Cl_2/hexane). The solvent was removed from the product containing fractions by rotary evaporation and oil pump vacuum to give five complexes as yellow solids: *trans,trans*-(C_6F_5)(*p*-tol$_3$P)$_2$Pt(C≡C)$_2$Pt(P*p*-tol$_3$)$_2$(C_6F_5) (**PtC$_4$Pt** [2a], 0.021 g, 0.011 mmol, 3%), *trans,trans*-(C_6F_5)(*p*-tol$_3$P)$_2$Pt(C≡C)$_2$Pt(P*p*-tol$_3$)(PPhMe$_2$)(C_6F_5) (**PtC$_4$Pt′-a**, 0.169 g, 0.0928 mmol, 23%), *trans,trans*-(C_6F_5)(*p*-tol$_3$P)$_2$Pt(C≡C)$_2$Pt(PPhMe$_2$)$_2$(C_6F_5) (**PtC$_4$Pt″-a**, 0.079 g, 0.048 mmol, 12%), *trans,trans*-(C_6F_5)(*p*-tol$_3$P)(Me$_2$PhP)Pt(C≡C)$_2$Pt(PPhMe$_2$)(P*p*-tol$_3$)(C_6F_5) (**Pt′C$_4$Pt′-a**, 0.184 g, 0.111 mmol, 27%), and *trans,trans*-(C_6F_5)(*p*-tol$_3$P)(Me$_2$PhP)Pt(C≡C)$_2$Pt(PPhMe$_2$)$_2$(C_6F_5) (**Pt′C$_4$Pt″-a**, 0.022 g, 0.015 mmol, 4%).

Data for **PtC$_4$Pt** [2a]. NMR (*δ*, $CDCl_3$): ^{1}H 7.42 (m, 24H, *o* to P), 6.88 (d, $^{3}J_{HH}$ = 7.8 Hz, 24H, *m* to P), 2.28 (s, 36H, CH_3); $^{31}P\{^{1}H\}$ 16.4 (s, $^{1}J_{PPt}$ = 2713 Hz [29]).

Data for **PtC$_4$Pt′-a.** mp 132 °C. Calcd for $C_{87}H_{74}F_{10}P_4Pt_2$ (1823.58): C, 57.30; H, 4.09. Found: 57.15; H, 4.22. NMR (*δ*, $CDCl_3$): ^{1}H 7.53 (m, 12H, *o* to P, tol, **Pt**), 7.37 (dd, $^{3}J_{HH}$ = 8.3 Hz, $^{3}J_{HP}$ = 11.2 Hz, 6H, *o* to P, tol, **Pt′**), 7.31–7.21 (m, 3H, *o*/*p* to P, Ph), 7.16–7.10 (m, 2H, *m* to P, Ph), 7.00 (d, $^{3}J_{HH}$ = 7.8 Hz, 12H, *m* to P, tol, **Pt**), 6.90 (dd, $^{3}J_{HH}$ = 8.4 Hz, $^{4}J_{HP}$ = 2.1 Hz, 6H, *m* to P, tol, **Pt′**), 2.30 (s, 18H, CH_3, tol, **Pt**), 2.28 (s, 9H, CH_3, tol, **Pt′**), 1.54 (dd, $^{2}J_{HP}$ = 10.5 Hz, $^{4}J_{HP}$ = 2.7 Hz, $^{3}J_{HPt}$ = 44.4 Hz [29], 6H, PMe_2); $^{13}C\{^{1}H\}$ [32,33] 146.4 (dd, $^{1}J_{CF}$ = 223 Hz, $^{2}J_{CF}$ = 26 Hz, *o* to **Pt′**, C_6F_5), 146.1 (dd, $^{1}J_{CF}$ = 222 Hz, $^{2}J_{CF}$ = 24 Hz, *o* to **Pt**, C_6F_5), 140.3 (s, *p* to P, tol, **Pt**), 140.1 (d, $^{4}J_{CP}$ = 2.3 Hz, *p* to P, tol, **Pt′**), 136.4 (dm, $^{1}J_{CF}$ = 267 Hz, *m*/*p* to **Pt/Pt′**, C_6F_5), 134.7 (virtual t [30], $^{2}J_{CP}$ = 6.3 Hz, *o* to P, tol, **Pt**), 134.5 (d, $^{2}J_{CP}$ = 11.5 Hz, *o* to P, tol, **Pt′**), 134.5 (dd, $^{1}J_{CP}$ = 59 Hz, $^{3}J_{CP}$ = 3.2 Hz, *i* to P, Ph), 130.2 (d, $^{2}J_{CP}$ = 9.1 Hz, *o* to P, Ph), 129.6 (d, $^{4}J_{CP}$ = 2.4 Hz, *p* to P, Ph), 128.5 (d, $^{3}J_{CP}$ = 10.7 Hz, *m* to P, tol, **Pt′**), 128.5 (virtual t [30], $^{3}J_{CP}$ = 5.4 Hz, *m* to P, tol, **Pt**), 128.3 (virtual t [30], $^{1}J_{CP}$ = 29.6 Hz, *i* to P, tol, **Pt**), 128.3 (dd, $^{1}J_{CP}$ = 55.4 Hz, $^{3}J_{CP}$ = 2.3 Hz, *i* to P, tol, **Pt′**), 128.0 (d, $^{3}J_{CP}$ = 10.0 Hz, *m* to P, Ph), 102.8 (s, $^{3}J_{CPt}$ = 31.5 Hz, $^{2}J_{CPt}$ = 266 Hz [29], PtC≡*C*), 100.8 (s, $^{3}J_{CP}$ = 33.8 Hz, $^{2}J_{CPt}$ = 273 Hz [29], Pt′C≡*C*), 88.8 (br, $^{1}J_{CPt}$ = 960 Hz [29], PtC/Pt′C), 21.5 (s, CH_3, tol, **Pt**), 21.4 (s, CH_3, tol, **Pt′**), 13.7 (dd, $^{1}J_{CP}$ = 38.2 Hz, $^{3}J_{CP}$ = 2.0 Hz, $^{2}J_{CPt}$ = 49.4 Hz [29], PMe_2); $^{31}P\{^{1}H\}$ 17.0 (s, $^{1}J_{PPt}$ = 2714 Hz [29], *p*-tol$_3$P, **Pt**), 15.9 (d, $^{2}J_{PP}$ = 436 Hz, $^{1}J_{PPt}$ = 2620 Hz [29], *p*-tol$_3$P, **Pt′**), −10.7 (d, $^{2}J_{PP}$ = 436 Hz, $^{1}J_{PPt}$ = 2554 Hz [29], Me$_2$PhP, **Pt′**).

Data for **PtC$_4$Pt″-a.** mp 101 °C. Calcd for $C_{74}H_{64}F_{10}P_4Pt_2$ (1657.38): C, 53.63; H, 3.89. Found: 53.82; H, 3.87. NMR (*δ*, $CDCl_3$): ^{1}H 7.55 (m, 12H, *o* to P, tol), 7.20 (m, 6H, *o*/*p* to P, Ph), 7.12 (d, 4H, $^{3}J_{HH}$ = 7.2 Hz, *m* to P, Ph), 7.08 (d, $^{3}J_{HH}$ = 7.8 Hz, 12H, *m* to P, tol), 2.36 (s, 18H, CH_3, tol), 1.55 (virtual t [30], $^{2}J_{HP}$ = 3.6 Hz, $^{3}J_{HPt}$ = 31.8 Hz [29], 12H, PMe); $^{13}C\{^{1}H\}$ 146.8 (dd, $^{1}J_{CF}$ = 229 Hz, $^{2}J_{CF}$ = 28 Hz, *o* to **Pt″**, C_6F_5), 146.1 (dd, $^{1}J_{CF}$ = 221 Hz, $^{2}J_{CF}$ = 25 Hz, *o* to **Pt**, C_6F_5), 140.4 (s, *p* to P, tol), 136.5 (dm, $^{1}J_{CF}$ = 266 Hz, *m*/*p* to **Pt/Pt″**, C_6F_5), 134.7 (virtual t [30], $^{2}J_{CP}$ = 6.3 Hz, *o* to P, tol), 134.1 (virtual t [30], $^{1}J_{CP}$ = 27.0 Hz, *i* to P, Ph), 130.2 (virtual t [30], $^{2}J_{CP}$ = 5.4 Hz, *o* to P, Ph), 129.7 (s, *p* to P, Ph), 128.6 (virtual t [30], $^{3}J_{CP}$ = 5.7 Hz, *m* to P, tol), 128.2 (virtual t [30], $^{1}J_{CP}$ = 29.9 Hz, *i* to P, tol), 128.1 (virtual t [30], $^{3}J_{CP}$ = 5.1 Hz, *m* to P, Ph), 124.8 (br, *i* to **Pt**, C_6F_5), 123.0 (br, *i* to **Pt″**, C_6F_5), 101.5 (s, $^{3}J_{CPt}$ = 34.7 Hz, $^{2}J_{CPt}$ = 260 Hz [29], PtC≡*C*), 97.5 (s, $^{3}J_{CP}$ = 33.2 Hz, $^{2}J_{CPt}$ = 286 Hz [29], Pt″C≡*C*), 89.1 (s, $^{1}J_{CPt}$ = 968 Hz [29], Pt″C), 88.9 (s, $^{1}J_{CPt}$ = 959 Hz [29], PtC), 21.6 (s, CH_3, tol), 14.0 (virtual t [30], $^{1}J_{CP}$ = 19.8 Hz, $^{2}J_{CPt}$ = 44.2 Hz [29], PMe_2); $^{31}P\{^{1}H\}$ 17.5 (s, $^{1}J_{PPt}$ = 2712 Hz [29], P(*p*-tol)$_3$), −10.8 (s, $^{1}J_{PPt}$ = 2458 Hz [29], Me$_2$PhP).

Data for **Pt′C$_4$Pt′-a.** mp 194 °C. Calcd for $C_{74}H_{64}F_{10}P_4Pt_2\cdot(CH_2Cl_2)_2$ (1827.20): C, 49.96; H, 3.75. Found: 50.29; H, 3.70. NMR (*δ*, $CDCl_3$): ^{1}H 7.46 (dd, $^{3}J_{HH}$ = 8.1 Hz, $^{3}J_{HP}$ = 11.1 Hz, 12H, *o* to P, tol, overlapped with m, 2H, *o* to P, Ph), 7.17–7.31 (m, 6H, *m*/*p* to P, Ph), 7.02 (d, $^{3}J_{HH}$ = 7.8 Hz, 12H, *m* to P, tol), 2.31 (s, 18H, CH_3, tol), 1.73 (dd, $^{2}J_{HP}$ = 10.5 Hz, $^{4}J_{HP}$ = 2.7 Hz, $^{3}J_{HPt}$ = 45 Hz [29], 12H, PMe_2); $^{13}C\{^{1}H\}$ 146.5 (dd, $^{1}J_{CF}$ = 223 Hz, $^{2}J_{CF}$ = 20 Hz, *o* to Pt, C_6F_5), 140.3 (d, $^{4}J_{CP}$ = 2.4 Hz, *p* to P, tol), 136.4 (dm, $^{1}J_{CF}$ = 282 Hz, *m*/*p* to Pt, C_6F_5), 134.6 (d, $^{2}J_{CP}$ = 11.1 Hz, *o* to P, tol), 134.4 (dd, $^{1}J_{CP}$ = 53 Hz, $^{3}J_{CP}$ = 3.1 Hz, *i* to P, Ph), 130.5 (d, $^{2}J_{CP}$ = 9.7 Hz, *o* to P, Ph), 129.8 (d, $^{4}J_{CP}$ = 2.4 Hz, *p* to P, Ph), 128.6 (d, $^{3}J_{CP}$ = 10.7 Hz, *m* to P, tol), 128.1 (d, $^{3}J_{CP}$ = 10.4 Hz, *m* to P, Ph), 128.2 (dd, $^{1}J_{CP}$ = 55.4 Hz, $^{3}J_{CP}$ = 2.7 Hz, $^{2}J_{CPt}$ = 26.2 Hz [29], *i* to P, tol), 126.1 (t, $^{2}J_{CF}$ = 50.4 Hz, *i* to Pt, C_6F_5), 99.6 (s, $^{3}J_{CPt}$ = 33.9 Hz, $^{2}J_{CPt}$ = 275 Hz [29], PtC≡*C*), 90.0 (s, $^{1}J_{CPt}$ = 971 Hz [29], Pt*C*), 21.5 (s, CH_3, tol), 14.2 (dd, $^{1}J_{CP}$ = 37.9 Hz, $^{3}J_{CP}$ = 2.0 Hz, $^{2}J_{CPt}$ = 45.0 Hz [29], PMe_2); $^{31}P\{^{1}H\}$ 16.8 (d, $^{2}J_{PP}$ = 435 Hz, $^{1}J_{PPt}$ = 2610 Hz [29], P(*p*-tol)$_3$), −10.8 (d,

$^2J_{PP}$ = 435 Hz, $^1J_{PPt}$ = 2570 Hz [29], Me_2PhP).

Data for **Pt′C$_4$Pt″-a.** NMR (δ, $CDCl_3$): ^{1}H 7.50 (dd, $^3J_{HH}$ = 8.0 Hz, $^3J_{HP}$ = 11.1 Hz, 6H, *o* to P, tol, **Pt′**, overlapped with m, 2H, *o* to P, Ph, **Pt′**), 7.32 (m, 6H, *o*/*p* to P, Ph, **Pt″**), 7.22 (m, 3H, *m*/*p* to P, Ph, **Pt′**), 7.12 (d, $^3J_{HH}$ = 8.4 Hz, 4H, *m* to P, Ph, **Pt″**), 7.07 (d, $^3J_{HH}$ = 8.1 Hz, 6H, *m* to P, tol), 2.33 (s, 9H, CH_3, tol), 1.88 (dd, $^2J_{HP}$ = 10.5 Hz, $^4J_{HP}$ = 2.7 Hz, $^3J_{HPt}$ = 45 Hz [29], 6H, PMe_2, **Pt′**), 1.70 (virtual t [30], $^2J_{HP}$ = 3.3 Hz, $^3J_{HPt}$ = 32.4 Hz [29], 12H, PMe_2, **Pt″**); ^{31}P{^{1}H} 18.0 (d, $^2J_{PP}$ = 433 Hz, $^1J_{PPt}$ = 2595 Hz [29], *p*-tol_3P), −10.2 (d, $^2J_{PP}$ = 433 Hz, $^1J_{PPt}$ = 2576 Hz [29], Me_2PhP, **Pt′**), −10.4 (s, $^1J_{PPt}$ = 2459 Hz [29], Me_2PhP, **Pt″**).

4.19. *trans,trans-*(C_6F_5)(*p*-tol_3P)((*p*-*t*-BuC_6H_4)$_2$PhP)Pt(C≡C)$_2$Pt(PPh(*p*-C_6H_4*t*-Bu)$_2$)(*Pp*-tol_3)(C_6F_5) (**Pt′C$_4$Pt′-b**). Synthesis A

A Schlenk flask was charged with **Pt′Cl-b** (0.286 g, 0.266 mmol), **Pt′C$_4$H-b** (0.289 g, 0.266 mmol), CuCl (0.014 g, 0.141 mmol), and $HNEt_2$ (60 mL). The mixture was stirred for 88 h at 45 °C. After cooling, the solvent was removed by oil pump vacuum, and the residue extracted with toluene (3 × 25 mL). The combined extracts were filtered through a neutral alumina column (8 cm, packed in toluene). The solvent was removed by rotary evaporation. The residue was chromatographed on a silica gel column (3.8 × 43 cm, 30:70 v/v CH_2Cl_2/hexane). The solvent was removed from the product containing fractions by rotary evaporation and oil pump vacuum to give three pure complexes as yellow solids: *trans*, *trans*-(C_6F_5)((*p*-*t*-BuC_6H_4)$_2$PhP)$_2$Pt(C≡C)$_2$Pt(PPh(*p*-C_6H_4*t*-Bu)$_2$)$_2$(C_6F_5) (**Pt″C$_4$Pt″-b**, 0.010 g, 0.005 mmol, 2%), *trans*,*trans*-(C_6F_5)(*p*-tol_3P)((*p*-*t*-BuC_6H_4)$_2$PhP)Pt(C≡C)$_2$Pt(PPh(*p*-C_6H_4*t*-Bu)$_2$)$_2$(C_6F_5) (**Pt′C$_4$Pt″-b**,0.036 g, 0.016 mmol, 6%) and **PtC$_4$Pt** (0.009 g, 0.005 mmol, 2%). Other fractions contained mixtures of three additional complexes. One of these (0.055 g) was chromatographed on a silica gel column (2.5 × 42 cm, 18:82 v/v ethyl acetate/hexane). The solvent was removed from the product containing fractions by rotary evaporation and oil pump vacuum to give *trans*,*trans*-(C_6F_5)(*p*-tol_3P)$_2$Pt(C≡C)$_2$Pt(PPh(*p*-C_6H_4*t*-Bu)$_2$)$_2$(C_6F_5) (**PtC$_4$Pt″-b**, 0.015 g, 0.007 mmol, 3%) and *trans*,*trans*-(C_6F_5)(*p*-tol_3P)$_2$Pt(C≡C)$_2$Pt(PPh(*p*-C_6H_4*t*-Bu)$_2$)(P*p*-tol_3)(C_6F_5) (**PtC$_4$Pt′-b**, 0.039 g, 0.019 mmol, 8%). Another fraction (0.064 g) was chromatographed on a silica gel column (2.5 × 43 cm, 12:88 v/v ethyl acetate/hexane). The solvent was removed from the product containing fractions by rotary evaporation and oil pump vacuum to give **Pt′C$_4$Pt″-b** (0.010 g, 0.005 mmol, 2%) and a mixture of **Pt′C$_4$Pt′-b** and **PtC$_4$Pt″-b** (0.050 g). NMR analysis of the mixture indicated 3% and 6% yields of **Pt′C$_4$Pt′-b** and **PtC$_4$Pt″-b**, respectively (a total of 0.046 g, 0.021 mmol, 8% for the latter).

Data for **Pt″C$_4$Pt″-b**. dec pt 205 °C. NMR (δ, $CDCl_3$): ^{1}H 7.75–7.67 (m, 8H, *o* to P, Ph), 7.44–7.35 (m, 16H, *o* to P, C_6H_4), 7.13 (d, $^3J_{HH}$ = 8.4 Hz, 16H, *m* to P, C_6H_4), 7.06 (m, 4H, *p* to P, Ph), 6.93 (m, 8H, *m* to P, Ph), 1.26 (s, 72H, $C(CH_3)_3$); ^{31}P{^{1}H} 16.0 (s, $^1J_{PPt}$ = 2715 Hz [29]).

Data for **Pt′C$_4$Pt″-b.** dec pt 182 °C. Calcd for $C_{115}H_{114}F_{10}P_4Pt_2$ (2200.19): C 62.78; H 5.22. Found: C 62.76, H 5.26. NMR (δ, $CDCl_3$): ^{1}H 7.77–7.66 (m, 6H, *o* to P, Ph), 7.48–7.36 (m, 18H, *o* to P, tol + C_6H_4), 7.14 (d, $^3J_{HH}$ = 8.4 Hz, 12H, *m* to P, C_6H_4, overlapped with m, 6H, *p* to P, Ph), 7.03–6.90 (m, 6H, *m* to P, Ph), 6.83 (d, $^3J_{HH}$ = 7.8 Hz, 6H, *m* to P, tol), 2.25 (s, 9H, CH_3, tol), 1.27 (s, 18H, $C(CH_3)_3$, **Pt′**), 1.26 (s, 36H, $C(CH_3)_3$, **Pt″**); ^{13}C{^{1}H} [32] 153.1 (s, *p* to P, C_6H_4, **Pt′** and **Pt″**), 146.0 (dd, $^1J_{CF}$ = 222 Hz, $^2J_{CF}$ = 24 Hz, *o* to Pt, C_6F_5), 139.9 (s, *p* to P, tol), 136.8 (dm, $^1J_{CF}$ = 235 Hz, *m*/*p* to Pt, C_6F_5), 135.02 (virtual t [30], $^2J_{CP}$ = 6.3 Hz, *o* to P, Ph, **Pt″**), 135.00 (virtual t [30], $^2J_{CP}$ = 6.2 Hz, *o* to P, Ph, **Pt′**), 134.6 (virtual t [30], $^2J_{CP}$ = 6.3 Hz, *o* to P, tol), 134.43 (virtual t [30], $^2J_{CP}$ = 5.8 Hz, *o* to P, C_6H_4, **Pt′**), 134.35 (virtual t [30], $^2J_{CP}$ = 6.0 Hz, *o* to P, C_6H_4, **Pt″**), 131.6 (dd, $^1J_{CP}$ = 30.6 Hz, $^3J_{CP}$ = 28.2 Hz, *i* to P, Ph, **Pt′**), 131.5 (virtual t [30], $^1J_{CP}$ = 29.0 Hz, *i* to P, Ph, **Pt″**), 129.8 (s, *p* to P, Ph, **Pt′** and **Pt″**), 128.3 (virtual t [30], $^3J_{CP}$ = 5.4 Hz, *m* to P, tol), 127.52 (virtual t [30], $^3J_{CP}$ = 5.0 Hz, *m* to P, Ph, **Pt′**), 127.47 (virtual t [30], $^3J_{CP}$ = 5.4 Hz, *m* to P, Ph, **Pt″**), 124.6 (virtual t [30], $^3J_{CP}$ = 5.4 Hz, *m* to P, C_6H_4, **Pt′** and **Pt″**), 104.4 (s, $^2J_{CPt}$ = 271 Hz [29], PtC≡*C*), 104.2 (s, $^2J_{CPt}$ = 271 Hz [29], PtC≡*C*), 87.0 (s, $^1J_{CPt}$ = 952 Hz [29], PtC), 34.8 (s, *C*(CH_3)$_3$), 31.38 (s, C(CH_3)$_3$, **Pt′**), 31.36 (s, C(CH_3)$_3$, **Pt″**), 21.5 (s, CH_3, tol); ^{31}P{^{1}H} [34], 16.35 (s, $^1J_{PPt}$ = 2713 Hz [29]), 16.16 (s, $^1J_{PPt}$ = 2712 Hz [29]).

Data for **PtC$_4$Pt″-b.** NMR (δ, $CDCl_3$): ^{1}H (see Fig. S5) [35] 7.75–7.65 (m, 4H, *o* to P, Ph), 7.48–7.35 (m, 20H, *o* to P, tol + C_6H_4), 7.14 (d, $^3J_{HH}$ = 7.5 Hz, 8H, *m* to P, C_6H_4, overlapped with m, 4H, *p* to P, Ph), 7.04–6.92 (m, 4H, *m* to P, Ph), 6.84 (dd, $^3J_{HH}$ = 7.8 Hz, $^4J_{HP}$ = 2.4 Hz, 12H, *m* to P, tol), 2.260, 2.251 (2 × s, 9H/9H, CH_3, tol), 1.264, 1.259 (2 × s, 18H/18H, $C(CH_3)_3$); ^{31}P{^{1}H} (see Fig. S6) [35] 16.2 (apparent t, J_{PP} = 17.2 Hz, $^1J_{PPt}$ = 2715 Hz [29]). MS (MALDI, THAP matrix, *m*/*z* for the most intense peak of the isotope envelope): 2130 (M^+, 46%), 2153 (M + Na^+, 74%), 2169 (M + K^+, 35%), and other peaks.

Data for **PtC$_4$Pt′-b.** dec pt 155 °C. Calcd for $C_{105}H_{94}F_{10}P_4Pt_2$ (2059.86): C, 61.22; H, 4.60. Found: C 61.27, H 4.73; NMR (δ, $CDCl_3$): ^{1}H 7.75–7.65 (m, 2H, *o* to P, Ph), 7.49–7.35 (m, 18H, *o* to P, tol + C_6H_4), 7.14 (d, $^3J_{HH}$ = 8.4 Hz, 4H, *m* to P, C_6H_4, overlapped with m, 2H, *p* to P, Ph), 7.02 (t, $^3J_{HH}$ = 7.6 Hz, 2H, *m* to P, Ph), 6.87 (d, $^3J_{HH}$ = 7.8 Hz, 18H, *m* to P, tol), 2.27 (s, 27H, CH_3, tol), 1.27 (s, 18H, $C(CH_3)_3$); ^{13}C{^{1}H} [32] 153.3 (s, *p* to P, C_6H_4, **Pt** and **Pt′**), 146.1 (dd, $^1J_{CF}$ = 223 Hz, $^2J_{CF}$ = 23 Hz, *o* to **Pt′**, C_6F_5), 140.04 (s, *p* to P, tol, **Pt′**), 140.00 (s, *p* to P, tol, **Pt**), 136.7 (dm, $^1J_{CF}$ = 218 Hz, *m*/*p* to **Pt′**, C_6F_5), 135.1 (virtual t [30], $^2J_{CP}$ = 6.7 Hz, *o* to P, Ph), 134.7 (virtual t [30], $^2J_{CP}$ = 6.2 Hz, *o* to P, tol, **Pt**/**Pt′**), 134.5 (virtual t [30], $^2J_{CP}$ = 6.1 Hz, *o* to P, C_6H_4), 131.7 (virtual t [30], $^1J_{CP}$ = 30 Hz, *i* to P, Ph), 129.9 (s, *p* to P, Ph), 128.4 (virtual t [30], $^3J_{CP}$ = 5.6 Hz, *m* to P, tol), 128.38 (virtual t [30], $^1J_{CP}$ = 29.7 Hz, *i* to P, tol, **Pt**), 128.35 (virtual t [30], $^1J_{CP}$ = 29.6 Hz, *i* to P, tol, **Pt′**), 128.1 (virtual t [30], $^1J_{CP}$ = 30.1 Hz, *i* to P, C_6H_4), 127.5 (virtual t [30], $^3J_{CP}$ = 5.4 Hz, *m* to P, Ph), 124.6 (virtual t [30], $^3J_{CP}$ = 5.4 Hz, *m* to P, C_6H_4), 104.4, 104.2 (2 × s, $^2J_{CPt}$ = 259/259 Hz [29], PtC≡*C*), 86.84, 86.60 (2 × s, $^1J_{CPt}$ = 970/965 Hz [29], PtC), 34.8 (s, *C*(CH_3)$_3$), 31.3 (s, CH_3), 21.4 (s, CH_3, tol); ^{31}P{^{1}H} 16.29 (s, $^1J_{PPt}$ = 2711 Hz [29], **Pt**), 16.17 (s, $^1J_{PPt}$ = 2712 Hz [29], **Pt′**).

4.20. Synthesis B

A Schlenk flask was charged with **Pt′Cl-b** (0.913 g, 0.848 mmol), **Pt′C$_4$H-b** (0.925 g, 0.848 mmol), CuCl (0.019 g, 0.194 mmol), *t*-BuOK (0.118 g, 1.048 mmol), KPF_6 (0.188 g, 1.023 mmol), THF (70 mL), and methanol (50 mL) with stirring. After 15 d, the solvent was removed by rotary evaporation and oil pump vacuum. The residue was extracted with CH_2Cl_2 (3 × 25 mL). The extract was filtered through a alumina/celite pad (2.5 × 5 cm). The solvent was removed by rotary evaporation and oil pump vacuum. The residue was chromatographed on a silica gel column (3.8 × 44 cm, 3:1 v/v toluene/hexane). The solvent was removed from the product containing fractions by rotary evaporation and oil pump vacuum to give two pure complexes, **Pt′C$_4$Pt″-b** (0.020 g, 0.009 mmol, 2%) and **Pt′Cl-b** (0.320 g, 0.297 mmol, 36%), as yellow and white solids, respectively. The other fractions were mixtures, and one that was rich in diplatinum products was chromatographed on a silica gel column (3.8 × 43 cm, 1:1 v/v chloroform/hexane). The solvent was removed from the product containing fractions by rotary evaporation and oil pump vacuum to give three pure complexes, **Pt′C$_4$H-b** (0.171 g, 0.157 mmol, 19%), **Pt′C$_4$Pt′-b** (0.379 g, 0.178 mmol, 21%) and **PtC$_4$Pt′-b** (0.014 g, 0.007 mmol, 1%).

Data for **Pt′C$_4$Pt′-b**. dec pt 165 °C. Calcd for $C_{110}H_{104}F_{10}P_4Pt_2$ (2130.09): C 62.03, H 4.92; found: C 62.13, H 4.96; NMR (δ, $CDCl_3$): ^{1}H 7.75–7.64 (m, 4H, *o* to P, Ph), 7.49–7.35 (m, 20H, *o* to P, tol + C_6H_4), 7.14 (d, $^3J_{HH}$ = 8.7 Hz, 8H, *m* to P, C_6H_4, overlapped with m, 4H, *p* to P, Ph), 7.05–6.95 (m, 4H, *m* to P, Ph), 6.83 (d,

$^3J_{HH}$ = 7.8 Hz, 12H, *m* to P, tol), 2.25 (s, 18H, CH_3, tol), 1.26 (s, 36H, $C(CH_3)_3$); $^{13}C\{^1H\}$ [32] 153.2 (s, *p* to P, C_6H_4), 146.1 (dd, $^1J_{CF}$ = 221 Hz, $^2J_{CF}$ = 21 Hz, *o* to Pt, C_6F_5), 140.0 (s, *p* to P, tol), 136.3 (dm, $^1J_{CF}$ = 254 Hz, *m*/*p* to Pt, C_6F_5), 135.0 (virtual t [30], $^2J_{CP}$ = 6.3 Hz, *o* to P, Ph), 134.6 (virtual t [30], $^2J_{CP}$ = 6.3 Hz, *o* to P, tol), 134.4 (virtual t [30], $^2J_{CP}$ = 5.9 Hz, *o* to P, C_6H_4), 131.7 (dd, $^1J_{CP}$ = 31.0 Hz, $^3J_{CP}$ = 27.6 Hz, *i* to P, Ph), 129.9 (s, *p* to P, Ph), 128.3 (virtual t [30], $^3J_{CP}$ = 5.5 Hz, *m* to P, tol), 128.3 (dd, $^1J_{CP}$ = 31.0 Hz, $^3J_{CP}$ = 28.4 Hz, *i* to P, tol), 128.1 (dd, $^1J_{CP}$ = 31.2 Hz, $^3J_{CP}$ = 27.8 Hz, *i* to P, C_6H_4), 127.5 (virtual t [30], $^3J_{CP}$ = 5.5 Hz, *m* to P, Ph), 124.6 (virtual t [30], $^3J_{CP}$ = 5.2 Hz, *m* to P, C_6H_4), 104.3 (s, $^2J_{CPt}$ = 254 Hz [29], PtC≡*C*), 86.8 (br s, $^1J_{CPt}$ = 967 Hz [29], Pt*C*), 34.9 (s, *C*$(CH_3)_3$), 31.4 (s, CH_3), 21.5 (s, CH_3, tol); $^{31}P\{^1H\}$ (see also Fig. S1) 16.4 (s, $^1J_{PPt}$ = 2711 Hz [29]).

4.21. *trans,trans-*$(C_6F_5)(p\text{-}tol_3P)((p\text{-}MeOC_6H_4)_2PhP)Pt(C{\equiv}C)_2Pt(PPh(p\text{-}C_6H_4OMe)_2)(Pp\text{-}tol_3)(C_6F_5)$ (**Pt′C$_4$Pt′-c**)

A Schlenk flask was charged with **Pt′Cl-c** (0.747 g, 0.729 mmol), **Pt′C$_4$H-c** (0.688 g, 0.663 mmol), CuCl (0.026 g, 0.263 mmol), and $HNEt_2$ (120 mL). The mixture was stirred for 88 h at 50 °C. After cooling, the solvent was removed by rotary evaporation. The maroon residue was chromatographed on a silica gel column (3.8 × 42 cm) using 40:60 v/v CH_2Cl_2/hexane to elute **PtC$_4$Pt** (0.022 g, 0.011 mmol, 2%), 50:50 v/v CH_2Cl_2/hexane to elute *trans*, *trans*-$(C_6F_5)(p\text{-}tol_3P)_2Pt(C{\equiv}C)_2Pt(Pp\text{-}tol_3)(PPh(p\text{-}C_6H_4OMe)_2)_2(C_6F_5)$ (**PtC$_4$Pt′-c**, 0.084 g, 0.042 mmol, 7%) and **PtCl** (0.111 g, 0.108 mmol, 16%), 60:40 v/v CH_2Cl_2/hexane to elute an unknown complex (0.062 g), *trans,trans*-$(C_6F_5)(p\text{-}tol_3P)_2Pt(C{\equiv}C)_2Pt(PPh(p\text{-}C_6H_4OMe)_2)_2(C_6F_5)$ (**PtC$_4$Pt″-c**, 0.059 g, 0.029 mmol, 5%), and *trans,trans*-$(C_6F_5)(p\text{-}tol_3P)((p\text{-}MeOC_6H_4)_2PhP)Pt(C{\equiv}C)_2Pt(PPh(p\text{-}C_6H_4OMe)_2)(Pp\text{-}tol_3)(C_6F_5)$ (**Pt′C$_4$Pt′-c**, 0.111 g, 0.055 mmol, 8%), 70:30 v/v CH_2Cl_2/hexane to elute **Pt′Cl-c** (0.199 g, 0.185 mmol, 26%), and 75:20 v/v CH_2Cl_2/hexane to elute *trans,trans*-$(C_6F_5)(p\text{-}tol_3P)((p\text{-}MeOC_6H_4)_2PhP)Pt(C{\equiv}C)_2Pt(PPh(p\text{-}C_6H_4OMe)_2)_2(C_6F_5)$ (**Pt′C$_4$Pt″-c**, 0.098 g, 0.048 mmol, 8%) and a second unknown complex (0.059 g).

Data for **PtC$_4$Pt′-c.** NMR (δ, $CDCl_3$): ^1H 7.57–7.35 (m, 24H, *o* to P, Ph + tol + C_6H_4), 7.16 (t, $^3J_{HH}$ = 7.8 Hz, 1H, *p* to P, Ph), 7.03 (t, $^3J_{HH}$ = 7.5 Hz, 2H, *m* to P, Ph), 6.88 (d, $^3J_{HH}$ = 7.8 Hz, 18H, *m* to P, tol), 6.62 (d, $^3J_{HH}$ = 8.7 Hz, 4H, *m* to P, C_6H_4), 3.73 (s, 6H, OCH_3), 2.28 (s, 27H, CH_3, tol); $^{31}P\{^1H\}$ 16.35 (s, $^1J_{PPt}$ = 2711 Hz [29], *p*-tol_3P, **Pt**), 16.24, 16.17 (2 × s, $^1J_{PPt}$ = 2707 Hz [29], *p*-tol_3P, (*p*-$MeOC_6H_4)_2$PhP, **Pt′**).

Data for **PtC$_4$Pt″-c.** dec pt 184 °C. Calcd for $C_{98}H_{80}F_{10}O_4P_4Pt_2$ (2025.68): C, 58.11; H, 3.98. Found: 58.10; H, 3.98. NMR (δ, $CDCl_3$): ^1H 7.54–7.36 (m, 24H, *o* to P, Ph + tol + C_6H_4), 7.18 (t, $^3J_{HH}$ = 7.2 Hz, 2H, *p* to P, Ph), 7.03 (t, $^3J_{HH}$ = 7.5 Hz, 4H, *m* to P, Ph), 6.90 (d, $^3J_{HH}$ = 7.8 Hz, 12H, *m* to P, tol), 6.63 (d, $^3J_{HH}$ = 9.0 Hz, 8H, *m* to P, C_6H_4), 3.73 (s, 12H, OCH_3), 2.29 (s, 18H, CH_3, tol); $^{13}C\{^1H\}$ [32] 161.1 (s, *p* to P, C_6H_4, **Pt′** and **Pt″**), 146.1 (dm, $^1J_{CF}$ = 229 Hz, *o* to **Pt/Pt″**, C_6F_5), 140.0 (s, *p* to P, tol), 136.4 (virtual t [30], $^2J_{CP}$ = 6.9 Hz, *o* to P, C_6H_4), 136.3 (dm, $^1J_{CF}$ = 261 Hz, *m*/*p* to **Pt/Pt″**, C_6F_5), 134.6 (virtual t [30], $^2J_{CP}$ = 6.3 Hz, *o* to P, tol), 134.0 (virtual t [30], $^2J_{CP}$ = 6.1 Hz, *o* to P, Ph), 132.4 (virtual t [30], $^1J_{CP}$ = 29.0 Hz, *i* to P, Ph), 129.7 (s, *p* to P, Ph), 128.3 (virtual t [30], $^3J_{CP}$ = 5.5 Hz, *m* to P, tol), 128.3 (virtual t [30], $^1J_{CP}$ = 29.6 Hz, *i* to P, tol), 127.4 (virtual t [30], $^3J_{CP}$ = 5.4 Hz, *m* to P, Ph), 122.2 (virtual t [30], $^1J_{CP}$ = 31.3 Hz, *i* to P, C_6H_4), 113.3 (virtual t [30], $^3J_{CP}$ = 5.8 Hz, *m* to P, C_6H_4), 104.1, 103.8 (2 × s, $^2J_{CPt}$ = 275 Hz [29], PtC≡*C*), 86.9 (br s, $^1J_{CPt}$ = 951 Hz [29], PtC≡C), 55.4 (s, OCH_3), 21.5 (s, CH_3, tol); $^{31}P\{^1H\}$ 16.30 (s, $^1J_{PPt}$ = 2710 Hz [29], Pp-tol_3), 15.92 (s, $^1J_{PPt}$ = 2698 Hz [29], (*p*-$MeOC_6H_4)_2$PhP).

Data for **Pt′C$_4$Pt′-c.** mp 128 °C. Calcd for $C_{98}H_{80}F_{10}O_4P_4Pt_2$ (2025.68): C, 58.11; H, 3.98. Found: 58.28; H, 3.89. NMR (δ, $CDCl_3$): ^1H 7.55–7.36 (m, 24H, *o* to P, Ph + tol + C_6H_4), 7.18 (t, $^3J_{HH}$ = 7.2 Hz, 2H, *p* to P, Ph), 7.04 (t, $^3J_{HH}$ = 7.2 Hz, 4H, *m* to P, Ph), 6.89 (d, $^3J_{HH}$ = 7.8 Hz, 12H, *m* to P, tol), 6.65 (d, $^3J_{HH}$ = 8.7 Hz, 8H, *m* to P, C_6H_4), 3.74 (s, 12H, OCH_3), 2.29 (s, 18H, CH_3); $^{13}C\{^1H\}$ [32] 161.1 (s, *p* to P, C_6H_4), 146.1 (dd, $^1J_{CF}$ = 223 Hz, $^2J_{CF}$ = 23 Hz, *o* to Pt, C_6F_5), 140.1 (s, *p* to P, tol), 136.4 (virtual t [30], $^2J_{CP}$ = 7.5 Hz, *o* to P, C_6H_4), 136.4 (dm, $^1J_{CF}$ = 258 Hz, *m*/*p* to Pt, C_6F_5), 134.6 (virtual t [30], $^2J_{CP}$ = 6.8 Hz, *o* to P, tol), 134.0 (virtual t [30], $^2J_{CP}$ = 6.5 Hz, *o* to P, Ph), 132.4 (dd, $^1J_{CP}$ = 33.4 Hz, $^3J_{CP}$ = 24.8 Hz, *i* to P, Ph), 129.7 (s, *p* to P, Ph), 128.4 (dd, $^3J_{CP}$ = 6.1 Hz, $^5J_{CP}$ = 4.8 Hz, *m* to P, tol), 128.3 (dd, $^1J_{CP}$ = 33.9 Hz, $^3J_{CP}$ = 25.4 Hz, *i* to P, tol), 127.4 (dd, $^3J_{CP}$ = 5.9 Hz, $^5J_{CP}$ = 4.6 Hz, *m* to P, Ph), 122.2 (dd, $^1J_{CP}$ = 36.0 Hz, $^3J_{CP}$ = 26.8 Hz, *i* to P, C_6H_4), 113.3 (dd, $^3J_{CP}$ = 6.6 Hz, $^5J_{CP}$ = 5.4 Hz, *m* to P, C_6H_4), 103.9 (s, $^2J_{CPt}$ = 264 Hz [29], PtC≡*C*), 86.8 (s, $^1J_{CPt}$ = 966 Hz [29], PtC≡C), 55.4 (s, OCH_3), 21.5 (s, CH_3, tol); $^{31}P\{^1H\}$ 16.17, 16.14 (2 × s, $^1J_{PPt}$ = 2704 Hz [29]).

Data for **Pt′C$_4$Pt″-c.** mp 119 °C. Calcd for $C_{97}H_{78}F_{10}O_6P_4Pt_2$ (2043.73): C, 57.01; H, 3.85. Found: 57.13; H, 3.86. NMR (δ, $CDCl_3$): ^1H 7.57–7.37 (m, 24H, *o* to P, Ph + tol + C_6H_4), 7.19 (t, $^3J_{HH}$ = 7.5 Hz, 3H, *p* to P, Ph), 7.05 (t, $^3J_{HH}$ = 7.2 Hz, 6H, *m* to P, Ph), 6.91 (d, $^3J_{HH}$ = 7.8 Hz, 6H, *m* to P, tol), 6.66 (d, $^3J_{HH}$ = 9.0 Hz, 4H, *m* to P, C_6H_4, **Pt′**), 6.65 (d, $^3J_{HH}$ = 8.7 Hz, 8H, *m* to P, C_6H_4, **Pt″**), 3.75 (s, 6H, OCH_3, **Pt′**), 3.74 (s, 12H, OCH_3, **Pt″**), 2.30 (s, 9H, CH_3); $^{13}C\{^1H\}$ [32] 161.1 (s, *p* to P, C_6H_4, **Pt′** and **Pt″**), 146.1 (dd, $^1J_{CF}$ = 223 Hz, $^2J_{CF}$ = 24 Hz, *o* to **Pt′/Pt″**, C_6F_5), 140.1 (s, *p* to P, tol), 136.4 (virtual t [30], $^2J_{CP}$ = 6.9 Hz, *o* to P, C_6H_4, **Pt′** and **Pt″**), 136.3 (dm, $^1J_{CF}$ = 261 Hz, *m*/*p* to **Pt′/Pt″**, C_6F_5), 134.6 (virtual t [30], $^2J_{CP}$ = 6.3 Hz, *o* to P, tol), 134.0 (virtual t [30], $^2J_{CP}$ = 6.1 Hz, *o* to P, Ph, **Pt′** and **Pt″**), 132.4 (virtual t [30], $^1J_{CP}$ = 29.0 Hz, *i* to P, Ph, **Pt″**), 132.4 (dd, $^1J_{CP}$ = 33.3 Hz, $^3J_{CP}$ = 25.0 Hz, *i* to P, Ph, **Pt′**), 129.7 (s, *p* to P, Ph, **Pt′** and **Pt″**), 128.4 (virtual t [30], $^3J_{CP}$ = 5.5 Hz, *m* to P, tol), 128.3 (dd, $^1J_{CP}$ = 33.6 Hz, $^3J_{CP}$ = 25.7 Hz, *i* to P, tol), 127.5 (virtual t [30], $^3J_{CP}$ = 5.4 Hz, *m* to P, Ph, **Pt′** and **Pt″**), 122.2 (dd, $^1J_{CP}$ = 35.9 Hz, $^3J_{CP}$ = 27.0 Hz, *i* to P, C_6H_4, **Pt′**), 122.2 (virtual t [30], $^1J_{CP}$ = 31.3 Hz, *i* to P, C_6H_4, **Pt″**), 113.3 (virtual t [30], $^3J_{CP}$ = 5.7 Hz, *m* to P, C_6H_4, **Pt′** and **Pt″**), 103.8, 103.7 (2 × s, $^2J_{CPt}$ = 265/265 Hz [29], PtC≡*C*), 87.0 (s, $^1J_{CPt}$ = 963 Hz [29], PtC≡C), 55.39 (s, OCH_3, **Pt′**), 55.37 (s, OCH_3, **Pt″**), 21.5 (s, CH_3, tol); $^{31}P\{^1H\}$ 16.19, 16.15 (2 × s, $^1J_{PPt}$ = 2703 Hz [29], *p*-tol_3P, (*p*-$MeOC_6H_4)_2$PhP, **Pt′**), 15.94 (s, $^1J_{PPt}$ = 2696 Hz [29], (*p*-$MeOC_6H_4)_2$PhP, **Pt″**).

4.22. *trans,trans-*$(C_6F_5)(p\text{-}tol_3P)(n\text{-}Pr_2PhP)Pt(C{\equiv}C)_2Pt(PPhn\text{-}Pr_2)(Pp\text{-}tol_3)(C_6F_5)$ (**Pt′C$_4$Pt′-d**)

A Schlenk flask was charged with **Pt′Cl-d** (0.876 g, 0.977 mmol), **Pt′C$_4$H-d** (0.888 g, 0.976 mmol), CuCl (0.021 g, 0.212 mmol), *t*-BuOK (0.146 g, 1.301 mmol), KPF_6 (0.239 g, 1.298 mmol), THF (70 mL), and methanol (50 mL) with stirring. After 92 h, the solvent was removed by rotary evaporation and oil pump vacuum. The residue was extracted with CH_2Cl_2 (3 × 25 mL). The extract was filtered through an alumina/celite pad (2.5 × 4 cm). The solvent was removed by rotary evaporation and oil pump vacuum. The residue was recrystallized twice from CH_2Cl_2 to yield pale yellow crystals of **Pt′C$_4$Pt′-d** (1.312 g, 0.741 mmol, 76%), dec pt 214 °C. Calcd for $C_{82}H_{80}F_{10}P_4Pt_2$ (1769.62): C, 55.66; H, 4.56. Found: 55.88; H, 4.72.

NMR (δ, $CDCl_3$): ^1H (see also Figs. S2 and S3) 7.46 (dd, $^3J_{HP}$ = 11.0 Hz, $^3J_{HH}$ = 8.0 Hz, 12H, *o* to P, tol), 7.41–7.34 (m, 4H, *o* to P, Ph), 7.27–7.21 (m, 2H, *p* to P, Ph), 7.20–7.15 (m, 4H, *m* to P, Ph), 6.99 (dd, $^3J_{HH}$ = 8.0 Hz, $^4J_{HP}$ = 2.0 Hz, 12H, *m* to P, tol), 2.31 (s, 18H, CH_3, tol), 2.20–2.08, 2.07–1.93 (2 × m, 4H/4H, PCH_2), 1.67–1.53, 1.47–1.33 (2 × m, 4H/4H, PCH_2CH_2), 0.87 (t, $^3J_{HH}$ = 7.5 Hz, 12H, $PCH_2CH_2CH_3$); $^{13}C\{^1H\}$ 146.5 (dd, $^1J_{CF}$ = 224 Hz, $^2J_{CF}$ = 25 Hz, *o* to Pt, C_6F_5), 140.2 (d, $^4J_{CP}$ = 2.4 Hz, *p* to P, tol), 136.6 (dm, $^1J_{CF}$ = 249 Hz, *m*/*p* to Pt, C_6F_5), 134.6 (d, $^2J_{CP}$ = 11.2 Hz, *o* to P, tol), 132.1 (dd, $^1J_{CP}$ = 49.1 Hz, $^3J_{CP}$ = 2.8 Hz, *i* to P, Ph), 131.3 (d, $^2J_{CP}$ = 8.8 Hz, *o* to P, Ph), 129.5 (d, $^4J_{CP}$ = 1.9 Hz, *p* to P, Ph), 128.5 (d, $^3J_{CP}$ = 10.8 Hz, *m* to P, tol), 128.4 (dd, $^1J_{CP}$ = 54.9 Hz, $^3J_{CP}$ = 3.0 Hz, *i* to P, tol), 127.9 (d, $^3J_{CP}$ = 9.7 Hz, *m* to P, Ph), 126.4 (t, $^2J_{CF}$ = 52.3 Hz, *i* to Pt, C_6F_5), 99.9 (s,

$^{2}J_{CPt}$ = 267.6 Hz [29], PtC≡*C*), 87.9 (br, $^{1}J_{CPt}$ = 971 Hz [29], Pt*C*≡C), 26.9 (dd, $^{1}J_{CP}$ = 33.5 Hz, $^{3}J_{CP}$ = 1.3 Hz, PCH_2), 21.4 (d, $^{5}J_{CP}$ = 1.1 Hz, CH_3, tol), 18.0 (s, PCH_2CH_2), 16.0 (d, $^{3}J_{CP}$ = 14.8 Hz, $PCH_2CH_2CH_3$); $^{31}P\{^{1}H\}$ 17.6 (d, $^{2}J_{PP}$ = 421 Hz, $^{1}J_{PPt}$ = 2620 Hz [29], *p*-tol_3P), 6.0 (d, $^{1}J_{PPt}$ = 2590 Hz [29], $^{2}J_{PP}$ = 421 Hz, *n*-Pr_2PhP).

4.23. Crystallography

Colorless crystals of **1** and **Pt′Cl-e** were grown from CH_2Cl_2/hexane at room temperature. Pale yellow crystals of **Pt′C_4H-a** were grown from CH_2Cl_2/acetone/hexane at -5 °C. Pale yellow crystals of **Pt′C_4Pt′-a**·$2CH_2Cl_2$ were grown from CH_2Cl_2/hexane at -5 °C. Orange-brown crystals of **PtC_4Pt″-b**·C_7H_8 were grown from toluene/ethanol at room temperature. Yellow crystals of **Pt′C_4Pt′-b** could be grown analogously, or from toluene/hexane at -15 °C (identical unit cells). Yellow crystals of **Pt′C_4Pt′-c** were grown from CH_2Cl_2/ethanol mixture at room temperature. Pale yellow crystals of **Pt′C_4Pt′-d** were grown from CH_2Cl_2 at −15 °C.

For all the data in Tables 1 and 2, integrated intensity information for each reflection was obtained by reduction of the data frames with the program APEX2 [36] or SAINTplus [37]. The integration method employed a three dimensional profiling algorithm, and all data were corrected for Lorentz and polarization factors, as well as crystal decay effects. These data were merged and scaled to produce suitable data sets. The program SADABS [38] was employed for absorption corrections. Structures were solved using SHELXTL (SHELXS) [39]. All non-hydrogen atoms were refined with anisotropic thermal parameters. Carbon bound hydrogen atoms were placed in idealized positions (C-H = 0.96 Å, $U_{iso}(H) = 1.2 \times U_{iso}(C)$). The structures were refined (weighted least squares/F^2) to convergence [39].

With **1**, the thermal parameters of the SC_4H_8 carbon atoms (C(45) to C(48)) indicated disorder, which could be modeled. The R factor (6.5%) and significant unaccounted electron densities near Pt(1) in the Fourier difference map (~6.4, 2.4, 1.8, and 1.6 eÅ^{-3}; distance from Pt(1) to highest *q*1 peak ca. 1.0 Å; distances between *q*1, *q*2, *q*3, and *q*4 all about 2.1 Å) suggested a "whole-molecule-disorder". Using O-fit in XP, the whole-molecule-disorder was modeled and refined, decreasing the R factor to 4.7%. There were two possible configurations for the disorder with the C_6F_5 ligands occupying opposite ends: one with both SC_4H_8 ligands and hence both Cl ligands occupying the same side, and the other with these ligands occupying opposite sides. Both models were refined, but the resulting R factors were very close and did not differentiate between them. The occupancy of the molecule with Pt(1) refined to 0.93, and that with Pt(1A) refined to 0.07. Considering the highly biased ratio, the refinement was carried out with the molecule with the minor occupancy fully rigid.

With **Pt′Cl-e**, systematic reflection conditions suggested the noncentrosymmetric space group $P2_12_12_1$. This assignment was further supported by statistical tests. With **Pt′C_4Pt′-a**·$2CH_2Cl_2$, there were no complications although the inversion center at the midpoint of the sp carbon chain is noteworthy.

With **PtC_4Pt″-b**·C_7H_8, the combination of the Cu source and the multi-wire detector on the GADDS diffractometer employed restricted the 2θ angle to 120°. This precluded attaining the resolution recommended by the CHECK-CIF protocol. Some *t*-Bu groups were disordered, but their occupancies could be modeled (73:27 for C(60/61/62) vs. C(60A/61A/62A); 46:54 for C(50/51/52) vs. C(50A/51A/52A); 24:76 for C(34/35/36) vs. C(34A/35A/36A)). Under the conditions employed, data collection could only be carried out to 93% completion.

With **Pt′C_4Pt′-b**, data were collected at the lowest temperature possible with the instrument (−60 °C, 213 K). Some *t*-Bu groups were disordered, but their occupancies could be modeled (61:39 for C(102/103/104) vs. C(130/131/132); 55:45 for C(49/50/51) vs. C(49A/C50A/C51A)). The fluorine atoms also exhibited elongated displacement parameters, suggesting a wagging of the C_6F_5 groups. No attempts were made to model this disorder.

With **Pt′C_4Pt′-c**, two methoxy groups were disordered over three sites: O(1)-C(38), O(2)-C(48), O(3)-C(51). As a result, one hydrogen on the phenyl group associated with this disorder is not modeled (the formula shows one less hydrogen). Some of the thermal parameters associated with the other methoxy groups are larger, but attempts to model additional disorder did not give lower R factors. The same limitations as with **PtC_4Pt″-b** precluded attaining the resolution recommended by the CHECK-CIF protocol.

With **Pt′C_4Pt′-d**, which exhibited an inversion center at the midpoint of the sp carbon chain, four carbon atoms of the phenyl group (C(34) to C(37)) and three of one *n*-propyl group (C(38) to C(40)) showed elongated thermal ellipsoids, indicating disorder. However, efforts to model this disorder did not improve the refinement.

Acknowledgement

The authors thank the US National Science Foundation (CHE-0719267, CHE-1153085, and CHE-1566601) for support.

Appendix A. Supplementary data

Supplementary data related to this article (NMR spectra showing non-first-order phenomena, space filling representations of molecular structures) can be found at http://dx.doi.org/10.1016/j.jorganchem.2017.05.006.

References

[1] (a) A. Klein, K.-W. Klinkhammer, T. Scheiring, J. Organomet. Chem. 578 (1999) 128–135;
(b) C. Müller, R.J. Lachicotte, W.D. Jones, Organometallics 21 (2002) 1190–1196;
(c) V.W.-W. Yam, K.M.-C. Wong, N. Zhu, Angew. Chem. Int. Ed. 42 (2003) 1400–1403. Angew. Chem. 115 (2003) 1438–1441.
[2] (a) W. Mohr, J. Stahl, F. Hampel, J.A. Gladysz, Chem. Eur. J. 9 (2003) 3324–3340;
(b) G.R. Owen, J. Stahl, F. Hampel, J.A. Gladysz, J. A. Chem. Eur. J. 14 (2008) 73–87;
(c) J. Stahl, J.C. Bohling, T.B. Peters, L. de Quadras, J.A. Gladysz, Pure Appl. Chem. 80 (2008) 459–474;
(d) L. de Quadras, A.H. Shelton, H. Kuhn, F. Hampel, K.S. Schanze, J.A. Gladysz, Organometallics 27 (2008) 4979–4991;
(e) G.R. Owen, S. Gauthier, N. Weisbach, F. Hampel, N. Bhuvanesh, J.A. Gladysz, Dalton Trans. 39 (2010) 5260–5271.
[3] Computational studies: (a) F. Zhuravlev, J.A. Gladysz, Chem. Eur. J. 10 (2004) 6510–6522;
(b) M. Samoc, M.G. Humphrey, G.T. Dalton, J.A. Gladysz, Q. Zheng, Y. Yelkov, H. Ågren, H.P. Norman, Inorg. Chem. 47 (2008) 9946–9957.
[4] (a) S. Takahashi, E. Murata, K. Sonogashira, N. Hagihara, Polym. Sci. Polym. Chem. Ed. 18 (1980) 661–669;
(b) W.-Y. Wong, C.-K. Wong, G.-L. Lu, K.-W. Cheah, J.-X. Shi, Z. Lin, J. Chem, Soc. Dalton Trans. 31 (2002) 4587–4594;
(c) L. Liu, W.-Y. Wong, S.-Y. Poon, J.-X. Shi, K.-W. Cheah, Z. Lin, Chem. Mater 18 (2006) 1369–1378.
[5] (a) T.B. Peters, J.C. Bohling, A.M. Arif, J.A. Gladysz, Organometallics 18 (1999) 3261–3263;
(b) W. Mohr, J. Stahl, F. Hampel, J.A. Gladysz, Inorg. Chem. 40 (2001) 3263–3264;
(c) J. Stahl, J.C. Bohling, E.B. Bauer, T.B. Peters, W. Mohr, J.M. Martín-Alvarez, F. Hampel, J.A. Gladysz, Angew. Chem. Int. Ed. 41 (2002) 1871–1876. Angew. Chem. 114(2002) 1951–1957;
(d) Q. Zheng, F. Hampel, J.A. Gladysz, Organometallics 23 (2004) 5896–5899;
(e) G.R. Owen, J. Stahl, F. Hampel, J.A. Gladysz, Organometallics 23 (2004) 5889–5892;
(f) Q. Zheng, J.A. Gladysz, J. Am, Chem. Soc. 127 (2005) 10508–10509;
(g) Q, J.C. Zheng, T.B. Bohling, A.C. Peters, F. Frisch, Hampel, J.A. Gladysz, Chem. Eur. J. 12 (2006) 6486–6505;
(h) L. de Quadras, F. Hampel, J.A. Gladysz, Dalton Trans. 35 (2006) 2929–2933;
(i) L. de Quadras, J. Stahl, F. Zhuravlev, J.A. Gladysz, J. Organomet. Chem. 692 (2007) 1859–1870;

(j) L. de Quadras, E.B. Bauer, J. Stahl, F. Zhuravlev, F. Hampel, J.A. Gladysz, New. J. Chem. 31 (2007) 1594–1604;
(k) J. Stahl, W. Mohr, L. de Quadras, T.B. Peters, J.C. Bohling, J.M. Martín-Alvarez, G.R. Owen, F. Hampel, J.A. Gladysz, J. Am. Chem. Soc. 129 (2007) 8282–8295;
(l) L. de Quadras, E.B. Bauer, W. Mohr, J.C. Bohling, T.B. Peters, J.M. Martín-Alvarez, F. Hampel, J.A. Gladysz, J. Am. Chem. Soc. 129 (2007) 8296–8309;
(m) R. Farley, Q. Zheng, J.A. Gladysz, K.S. Schanze, Inorg. Chem. 47 (2008) 2955–2963;
(n) S. Ballmann, W. Hieringer, D. Secker, Q. Zheng, J.A. Gladysz, A. Görling, H.B. Weber, Chem. Phys. Chem. 11 (2010) 2256–2260;
(o) N. Weisbach, Z. Baranová, S. Gauthier, J.H. Reibenspies, J.A. Gladysz, Chem. Commun. 48 (2012) 7562–7564;
(p) H. Sahnoune, Z. Baranová, N. Bhuvanesh, J.A. Gladysz, J.-F. Halet, Organometallics 32 (2013) 6360–6367;
(q) Z. Baranová, H. Amini, N. Bhuvanesh, J.A. Gladysz, Organometallics 33 (2014) 6746–6749;
(r) Y. Li, R.W. Winkel, N. Weisbach, J.A. Gladysz, K.S. Schanze, J. Phys, Chem. A 115 (2014) 10333–10339.

[6] (a) S. Szafert, J.A. Gladysz, Chem. Rev. 103 (2003) 4175–4205;
(b) S. Szafert, J.A. Gladysz, Chem. Rev. 106 (2006) PR1–PR33.

[7] For other metal polyynediyl complexes that exhibit more stable radical cations at shorter sp chain lengths, see: (a) M. Brady, W. Weng, Y. Zhou, J.W. Seyler, A.J. Amoroso, A.M. Arif, M. Böhme, G. Frenking, J.A. Gladysz, J. Am. Chem. Soc. 119 (1997) 775–788;
(b) W.E. Meyer, A.J. Amoroso, C.R. Horn, M. Jaeger, J.A. Gladysz, Organometallics 20 (2001) 1115–1127.

[8] T. Zhang, N. Bhuvanesh, J.A. Gladysz, Eur. J. Inorg. Chem. 2017 (2017) 1017–1025.

[9] (a) E.L. Eliel, S.H. Wilen, Stereochemistry of Organic Compounds, John Wiley & Sons, New York, 1994 (Chapter 14);
(b) G. Bringmann, A.J.P. Mortimer, P.A. Keller, M.J. Gresser, J. Garner, B. Breuning, Angew. Chem. Int. Ed. 44 (2005) 5384–5427. Angew. Chem. 117 (2005) 5518–5563;
(c) J. Clayden, W.J. Moran, P.J. Edwards, S.R. LaPlante, Angew. Chem. Int. Ed. 121 (2009) 6398–6401. Angew. Chem. 48(2009) 6516–6520;
(d) E. Kumarasamy, R. Raghunathan, M. Sibi, J. Sivaguru, Chem. Rev. 115 (2015) 11239–11300.

[10] (a) H. Ogawa, T. Joh, S. Takahashi, K. Sonogashira, J. Chem, Soc. Chem. Commun. (1985) 1220–1221;
(b) H. Ogawa, K. Onitsuka, T. Joh, S. Takahashi, Organometallics 7 (1988) 2257–2260;
(c) J.R. Berenguer, J. Forniés, E. Lalinde, F. Martínez, Organometallics 14 (1995) 2532–2537;
(d) C.S. Griffith, G.A. Koutsantonis, Aust. J. Chem. 65 (2012) 698–722.

[11] Throughout this manuscript, the descriptor *trans* refers to the orientation of the two phosphine ligands at platinum.

[12] A.J. Cheney, B.E. Mann, B.L. Shaw, R.M. Salde, J. Chem. Soc. A (1971) 3833–3842.

[13] S.O. Grim, R.L. Keiter, W. McFarlane, Inorg. Chem. 6 (1967) 1133–1137.

[14] C.M. DiMeglio, L.A. Luck, C.D. Rithner, A.L. Rheingold, W.L. Elcesser, J.L. Hubbard, C.H. Bushweller, J. Phys. Chem. 94 (1990) 6255–6263.

[15] R. Usón, J. Forniés, F. Martinez, M. Tomás, J. Chem. Soc. Dalton Trans. 9 (1980) 888–894.

[16] (a) G.B. Deacon, K.T. Nelson-Reed, J. Organomet. Chem. 322 (1987) 257–268;
(b) Better results were obtained when this compound was synthesized by a procedure previously applied to *p*-tol or *p*-C_6H_4OMe analogs; see S. Shekhar, J.F. Hartwig, J. Am. Chem. Soc. 126 (2004) 13016–13027.

[17] S. Dey, Final Research Report, Texas A&M University, 2011.

[18] The ligands *p*-tol_3P, (*p*-*t*-$BuC_6H_4)_2PhP$, and (*p*-$MeOC_6H_4)_2PhP$ would be expected to have similar steric and electronic properties. One manifestation of the latter is the close correspondence of the average of the ó values for the three *para* substituents (−0.14, −0.10, −0.19, respectively; data from M.B. Smith, J. March, March's Advanced Organic Chemistry, John Wiley & Sons, New York, 2007; Table 9.4).

[19] W.H. Hersh, J. Chem. Educ. 74 (1997) 1485–1488.

[20] (a) F. Ponzini, R. Zagha, K. Hardcastle, J.S. Siegel, Angew. Chem. Int. Ed. 39 (2000) 2323–2325. Angew. Chem. 112 (2000) 2413–2415;
(b) M.D. Blanchard, R.P. Hughes, T.E. Concolino, A.L. Rheingold, Chem. Mater 12 (2000) 1604–1610;
(c) H. Adams, J.-L. Jimenez Blanco, G. Chessari, C.A. Hunter, C.M.R. Low, J.M. Sanderson, J.G. Vinter, Chem. Eur. J. 7 (2001) 3494–3503;
(d) B.W. Gung, J.C. Amicangelo, J. Org. Chem. 71 (2006) 9261–9270.

[21] J.S. Siegel, F.A.L. Anet, J. Org. Chem. 53 (1988) 2629–2630.

[22] W.C. Trogler, Int. J. Chem. Kinet. 19 (1987) 1025–1047.

[23] (a) J.A. Ramsden, W. Weng, A.M. Arif, J.A. Gladysz, J. Am. Chem. Soc. 114 (1992) 5890–5891;
(b) W. Weng, T. Bartik, M. Brady, B. Bartik, J.A. Ramsden, A.M. Arif, J.A. Gladysz, J. Am. Chem. Soc. 117 (1995) 11922–11931.

[24] (a) A.C. Albéniz, A.L. Casado, P. Espinet, P. Organometallics 16 (1997) 5416–5423;
(b) M.L. Zanini, M.R. Meneghetti, G. Ebeling, P.R. Livotto, F. Rominger, J. Dupont, Inorg. Chim. Acta 350 (2003) 527–536;
(c) R.E. Andrew, D.W. Ferdani, C.A. Ohlin, A.B. Chaplin, Organometallics 34 (2015) 913–917.

[25] H.S. Chow, E.C. Constable, R. Frantz, C.E. Housecroft, J. Lacour, M. Neuburger, C.D. Rappoport, S. Schaffner, New. J. Chem. 33 (2009) 376–385.

[26] C. Eaborn, K.J. Odell, A. Pidcock, J. Chem. Soc. Dalton Trans. 7 (1978) 357–368.

[27] L. Caron, M. Canipelle, S. Tilloy, H. Bricout, E. Monflier, Tetrahedron Lett. 42 (2001) 8837–8840.

[28] H.D. Verkruijsse, L. Brandsma, Synth. Commun. 21 (1991) 657–659.

[29] This coupling represents a satellite (d, $^{195}Pt = 33.8\%$) as is not reflected in the peak multiplicity given.

[30] There are many non-first-order couplings evident in the NMR spectra, especially with complexes with different triarylphosphine ligands on the same platinum, as further discussed in the text. In some cases, virtual triplets are observed, and in other cases doublet of doublets with nearly the same *J* values as the triplets. In both cases, the *J* values represent the apparent couplings between adjacent peaks and not the mathematically rigorously coupling constants [19].

[31] (a) The phosphorus and sulfur donor ligands in **1** are *cis*.
(b) tht = tetrahydrothiophene.

[32] One or more of the arene signals *ipso* to phosphorus (P) or platinum (Pt) were not observed.

[33] This spectrum was recorded using single crystals grown from acetone/diethyl ether/CH_2Cl_2/hexane. Signals (δ) for acetone (207.2, 31.1), diethyl ether (66.0, 15.5), and CH_2Cl_2 (53.7) were apparent.

[34] The signal intensities are similar and do not allow an unambiguous assignment (theory, 2:1:1).

[35] Although the NMR spectra of **PtC_4Pt''-b** exhibit some unusual non-first order features, the structural assignment is unequivocal, as evidenced by the mass spectrum and crystallographic data (Figure 8).

[36] APEX2 "Program for Data Collection on Area Detectors" BRUKER AXS Inc., 5465 East Cheryl Parkway, Madison, WI 53711–5373 USA.

[37] SAINT (Version 7). "Program for Data Integration from Area Detector Frames", Bruker–Nonius Inc., 5465 East Cheryl Parkway, Madison, WI 53711–55373 (USA).

[38] F. Paul, C. Lapinte, in: M. Gielen, R. Willem, B. Wrackmeyer (Eds.), Unusual Structures and Physical Properties in Organometallic Chemistry, Wiley, New York, 2002, pp. 220–291.

[39] G.M. Sheldrick, Acta Cryst. A64 (2008) 112–122.